Check for updates

Recent Advances of Bioresponsive Nano-Sized Contrast Agents for Ultra-High-Field Magnetic Resonance Imaging

Hailong Hu [1,2]*

[1] School of Aeronautics and Astronautics, Central South University, Changsha, China, [2] Research Center in Intelligent Thermal Structures for Aerospace, Central South University, Changsha, China

The ultra-high-field magnetic resonance imaging (MRI) nowadays has been receiving enormous attention in both biomaterial research and clinical diagnosis. MRI contrast agents are generally comprising of T_1-weighted and T_2-weighted contrast agent types, where T_1-weighted contrast agents show positive contrast enhancement with brighter images by decreasing the proton's longitudinal relaxation times and T_2-weighted contrast agents show negative contrast enhancement with darker images by decreasing the proton's transverse relaxation times. To meet the incredible demand of MRI, ultra-high-field T_2 MRI is gradually attracting the attention of research and medical needs owing to its high resolution and high accuracy for detection. It is anticipated that high field MRI contrast agents can achieve high performance in MRI imaging, where parameters of chemical composition, molecular structure and size of varied contrast agents show contrasted influence in each specific diagnostic test. This review firstly presents the recent advances of nanoparticle contrast agents for MRI. Moreover, multimodal molecular imaging with MRI for better monitoring is discussed during biological process. To fasten the process of developing better contrast agents, deep learning of artificial intelligent (AI) can be well-integrated into optimizing the crucial parameters of nanoparticle contrast agents and achieving high resolution MRI prior to the clinical applications. Finally, prospects and challenges are summarized.

Keywords: nano-sized, contrast agents, magnetic resonance imaging, multimodal imaging, artificial intelligence

INTRODUCTION

As one of the most attractive and useful techniques for non-invasive imaging, magnetic resonance imaging (MRI) shows its great superiority in the practical application of clinic diagnosis, as well as the biomedical research (Zhao et al., 2001, 2013, 2015; Werner et al., 2008; Kim et al., 2009; Lee et al., 2012; Bao et al., 2018; Pellico et al., 2019; Liu et al., 2020). It is well-acknowledged that spatial resolution can be promoted by high magnetic field over 3 T, demonstrating a high signal-to-noise ratio (Vaughan et al., 2009; Rosenberg et al., 2010; Zhou et al., 2015b; Ni et al., 2016; Zhang et al., 2016). This result is usually evidenced by the MRI study on small animals under the applied high field (over 7 T) (Nakada, 2007; Werner et al., 2008; Faucher et al., 2012; Ni et al., 2016). Moreover, compared with 1.5 or 3.0 T MRI, ultra-high-field MRI shows its unique advantage in medical imaging, especially in the field neuroscience, where functional brain responses can be

FIGURE 1 | Relationship between structure and relaxivity of nanoparticle contrast agent for MRI. **(A)** Schematic diagram of mechanism for contrast agents (Ni et al., 2017); Copyright 2017, reproduced with permission from The Royal Society of Chemistry **(B)** factors illustrated for affecting contrast agent's relaxivity (Verwilst et al., 2015); Copyright 2015, reproduced with permission from The Royal Society of Chemistry. **(C)** Efficient chemical exchange for protons to accelerate T_1 relaxation (Zhou et al., 2015a); Copyright 2015, reproduced with permission from American Chemical Society **(D)** surface modification of nanoparticles contributing to MRI T_2 contrast agents (Zhang et al., 2016); Copyright 2016, reproduced with permission from American Chemical Society.

non-invasively measured with increasing sensitivity and greater spatial resolution under ultra-high-field MRI (de Martino et al., 2018). However, much more effort should be devoted to exploring the ultra-high-field MRI to eventually achieve the enhanced solution and sensitivity for clinical imaging diagnosis (Duyn, 2012; Zhao et al., 2013; Chang et al., 2016; Gautam et al., 2019; Harris et al., 2019; Rajamanickam, 2019).

The lanthanide ions such as Dy^{3+} and Ho^{3+} contrast agent ions are generally used for high magnetic field MRI (Das et al., 2011, 2012; Harris et al., 2016; Ni et al., 2016; Zhang et al., 2016). Signal intensity of MRI is affected by the relaxation rate of *in vivo* water protons. By using the contrast agent with varied contents, the MRI signal intensity can be changed, where paramagnetic metal ion in contrast agent with different concentrations will positively alter the relaxation rate of nearby water proton spins (Idisi et al., 2019; Kubíčková et al., 2019). The contrast agent for MRI has been illustrated in **Figure 1**, where several factors affecting the MRI have been clearly indicated with the listed examples. **Figure 1A** shows the general mechanism of contrast agent, where the change of hydrogen atom's magnetization in water plays a predominant role in deciding the capability of generated contrast for contrast agent. For the atomic structure of paramagnetic contrast agent,

paramagnetic center, inner sphere, secondary sphere and outer sphere are included. The relaxation contribution is quantitatively determined by the location between water protons and contrast agent. Water molecules coordinated to paramagnetic center will contribute to the inner sphere relaxation contribution and bulk water molecules will be responsible for the outer sphere relaxation (Ni et al., 2017; Marasini et al., 2020).

Moreover, take the gadolinium ions based contrast agent as another case, surface modification of organic ligands will be tightly binding to gadolinium ion avoid the toxicity for clinical diagnosis (Csajbok et al., 2005; Bridot et al., 2007). For this case, the hydrogen are bonded to the ligand instead of water molecules bounding to gadolinium ion, forming the second sphere in **Figure 1B** (Verwilst et al., 2015). Other crucial factors to the relaxation mechanism of contrast agent, such as chemical structure and surface modification (Zhu et al., 2016; Wang et al., 2018; Jin et al., 2019; Yin et al., 2019; Zhang et al., 2019) are also illustrated (**Figures 1C,D**), where efficient chemical exchange for protons accelerates relaxation and surface modification of nanoparticles contributes to MRI T_2 contrast agents, respectively (Zhou et al., 2015a; Zhang et al., 2016). Specifically, the effect of particle size and magnetic field on influencing relaxivities of r_1 and r_2 has been investigated based on the out-sphere theory,

showing the increased r_2 contributed by the increasing core size, decreasing coating layer thickness or increasing magnetic field.

When employing contrast agents for MRI, contrast agent shall possess the following distinct features for better imaging (Zhou et al., 2019): (a) Nano-size, achieve the maximum recognition; (b) diagnosis with high accuracy; (c) Compatibility, non-cytotoxic and biocompatible; (d) Stability, both chemical and photochemical stable; (e) Metabolism; renal excretion from body (Qin et al., 2007; Huang et al., 2010; Botar et al., 2020).

In addition, the recent progress of emerging artificial intelligence (AI) has advanced the exploration of ultra-high-field MRI, where AI in conjunction with MRI is supposed to be prevalently used in many cases, ranging from imaging reconstruction to the final clinical decision support (Busch, 2019). For instance, Sheth et al. discussed the AI in interpreting breast cancer on MRI, aiming to enhance the efficacy and accuracy of diagnosis (Sheth and Giger, 2019). To bridge the current gap between virtual reality and neuropathology, AI and ultra-high-field MRI with enhanced resolution will inevitably advance the knowledge of microstructure changes in varied pathogenetic stages (O'sullivan et al., 2019).

RECENT ADVANCES OF CONTRAST AGENTS FOR ULTRA-HIGH-FIELD MRI

To reveal the efficacy of a variety of contrast agents, crucial parameters have been defined to indicate the efficiency and species of contrast agents. Transverse relaxivity (r_2), longitudinal relaxivity (r_1) and the ratio of r_2/r_1 are used to evaluate the contrast efficiency of MRI contrast agent, where a high ratio of r_2/r_1 generally results in a high contrast efficiency (Shen et al., 2017b). A more efficient T_2 contrast agent instead of T_1 contrast agent will be determined by the increasing ratio of r_2/r_1 (Das et al., 2012). Metal ion includes the electron orbital motion and electron spin motion. The electron spin magnetic moment plays a predominant role in determining the longitudinal water relaxation (r_1). The existence of electron spin angular momentum of adjacent ions contributes to an enlarged total electron angular momentum, leading to a high r_1. On the contrary, total electron angular momentum will be quite small if contribution is only from electron orbital angular momentum.

Gadolinium chelates are commonly used as contrast agents owing to its advantages of offering superior non-invasive visualization for ailments (Rogosnitzky and Branch, 2016; Marangoni et al., 2017; Rees et al., 2018; Clough et al., 2019). However, both the short circulation lifetime in the body and the relatively low proton relaxation efficiency substantially limit its wide application. Moreover, to achieve the high proton relaxation efficiency, high concentration of contrast agents is required, which will deteriorate human's body in terms of the side effect induced by Gd^{3+} ions.
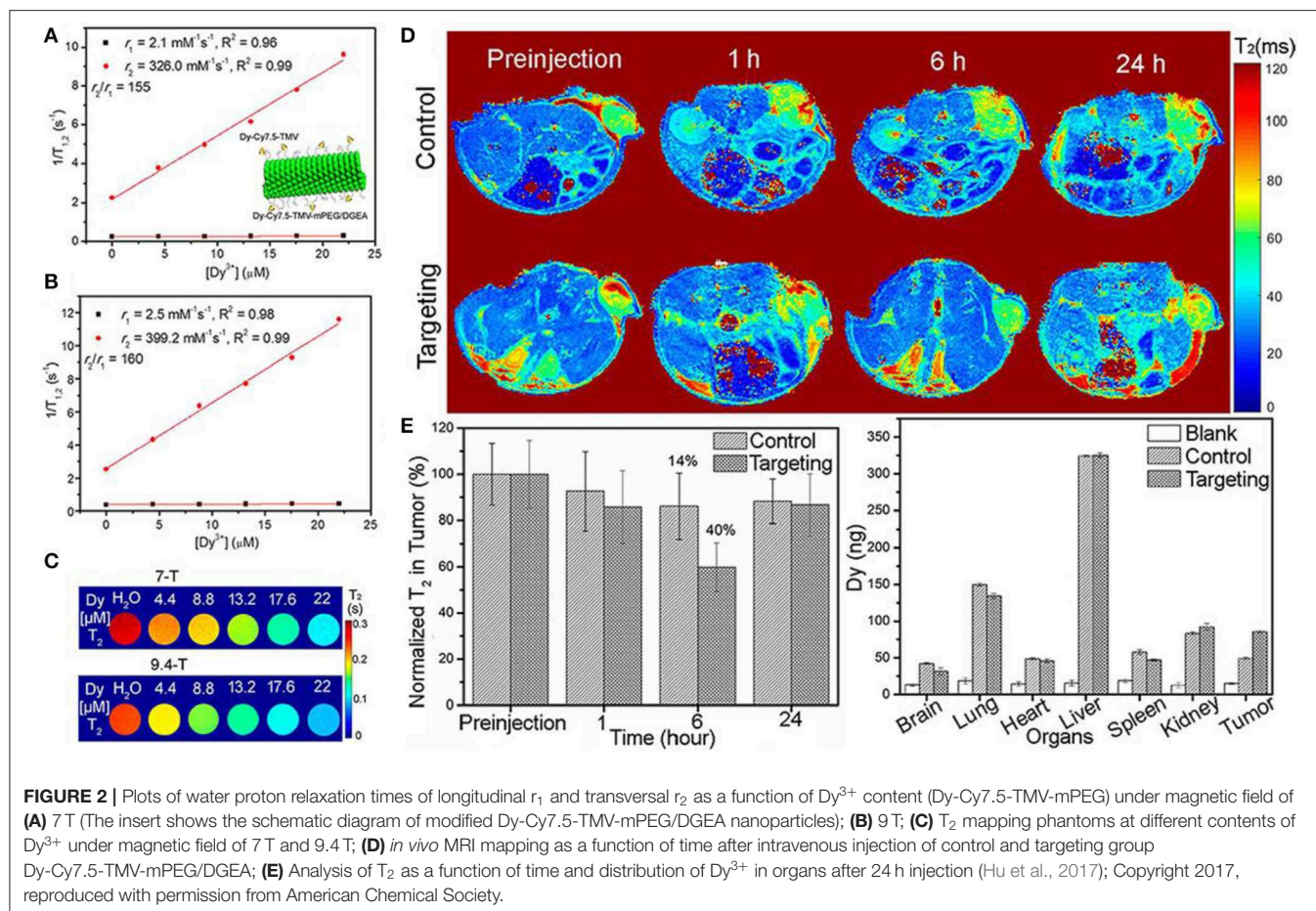
Alternatively, nanoparticle with magnetic responsive atom is becoming one of the most promising candidates to be used as contrast agents, such as transition metal ions (Cu^{2+}, Fe^{2+}/Fe^{3+},Co^{2+}, and Mn^{2+}, lanthanide metal ions (Eu^{3+}, Gd^{3+},

Ho^{3+}, and Dy^{3+}) (Tromsdorf et al., 2007; Mahmoudi et al., 2011; Busquets et al., 2015; Ni et al., 2017; Sousa et al., 2017; Guo et al., 2019; Hai et al., 2019; Wahsner et al., 2019; Botar et al., 2020). Furthermore, iron-based nano-system is highly recommended as spin-spin imaging or imaging probe because of its merits of electronic, magnetic, optical properties at nano scale and the excellent *in vivo* stability as well (Li et al., 2013). On the other hand, high surface area of nanoparticle promotes the chemical reactivity and make it viable to be modified with the biological and bioactive surfactants. Therefore, owing to these superior benefits, nanoparticles have been regarded as one of the promising alternatives for imaging contrast agents in future (Bobo et al., 2016; Chen et al., 2016; Shen et al., 2017c).

It is well-recognized that ultra-high-field MRI has achieved the increasing prevalence in both fundamental research and clinical applications (Dyke et al., 2017; Huelnhagen et al., 2017; Lehericy et al., 2017; Hametner et al., 2018). A bimodal contrast agent of Dy^{3+}(DOTA)/Cy7.5-conjugated tobacco mosaic virus (TMV) was developed for ultra-high-field MRI, confirming its high transverse relaxivity r_2 and suitable for both NIRF imaging and T_2 MRI in cancel cells diagnosis (Hu et al., 2017). **Figures 2A,B** show the relaxivity of contrast agent under ultra-high-magnetic of 7.0 and 9.4 T. Both high r_2 and high ratio of r_2/r_1 are obtained, showing the high efficiency of T_2 contrast agent for ultra-high-field MRI application. To further confirm the feasibility of this contrast agent, experiments are performed on concentration dependent phantom images (T_2-mapping) of contrast agent in water solutions at 7.0 and 9.4 T, showing a pronounced negative contrast gradient as a function of contrast agent concentration (**Figure 2C**). Till now, this kind of contrast agent demonstrates its great potential for ultra-high-field MRI. Furthermore, this contrast agent is to target tumors of mouse models by *in vivo* T_2-mapping MRI to check its ability. The impact of targeted and untargeted nanoparticles on local tissues is determined based on the relaxation times. **Figure 2D** shows a much stronger signal enhancement after contrast agent postinjection for a certain of hours (6 h) and the recovery is achieved after T_2 relaxation of 24 h. The biodistribution of nanoparticle contrast agent in organs and tumors are also determined (**Figure 2E**), showing more targeted nanoparticles accumulated in the tumors of mice than that of control nanoparticles, which is well-consistent with *in vivo* MRI images. Moreover, a certain number of nanoparticles are expected to stay in the liver owing to circulation of mononuclear phagocytic system. Consequently, the *in vivo* MRI results of nanoparticle confirm its efficiency as contrast agent.

Ni et al. prepared the $NaHoF_4$ nanoparticles via surface modification and studied the size effect of nanoparticles on MRI contrast agent performance under varied magnetic fields (**Figure 3**) (Ni et al., 2016, 2017). The optimal size of nanoparticles has been eventually achieved to test ultra-high-field MRI, showing an excellent biocompatibility and great promising candidate for future high field MRI. Moreover, as the size change of nanoparticles will bring alterable performance to MRI, whose detailed mechanism are also investigated, demonstrating

FIGURE 2 | Plots of water proton relaxation times of longitudinal r_1 and transversal r_2 as a function of Dy^{3+} content (Dy-Cy7.5-TMV-mPEG) under magnetic field of **(A)** 7 T (The insert shows the schematic diagram of modified Dy-Cy7.5-TMV-mPEG/DGEA nanoparticles); **(B)** 9 T; **(C)** T_2 mapping phantoms at different contents of Dy^{3+} under magnetic field of 7 T and 9.4 T; **(D)** in vivo MRI mapping as a function of time after intravenous injection of control and targeting group Dy-Cy7.5-TMV-mPEG/DGEA; **(E)** Analysis of T_2 as a function of time and distribution of Dy^{3+} in organs after 24 h injection (Hu et al., 2017); Copyright 2017, reproduced with permission from American Chemical Society.

the predominant curie mechanism for size below 7 nm and the main contribution of dipolar mechanism for size over 7 nm. Both rod-like $NaDyF_4$ and $NaHoF_4$ nanoparticles were prepared via a high temperature synthesis process and they are the promising candidate as T_2 contrast agents under the high field of 9.4 T MRI. Simulation results indicate the increase of 100 times for relaxivity when magnetic field increases from 1 to 10 T. Parameter such as the size was also studied and showed an increase of 30 times for both r_1 and r_2 when nanoparticle core size increases from 5 to 15 nm (Zhang et al., 2016).

Except the contrast agent developed for T_2-weighted MRI, the attempts into developing dual-mode T_1/T_2 contrast agents are also reported. Biju et al. reported a new type of contrast agent which can be used in either ultra-high magnetic field or multimodal imaging of MRI and optical imaging (Biju et al., 2018). This kind of contrast agent NP-PAA-FA is designed with core-shell structure with an average size of about 24 nm, and surface modification/functionalization is applied to enhance the contrast agent's biocompatibility. Both MRI and proton nuclear magnetic relaxation dispersion studies confirm the contrast agent's feasibility of behaving as a dual-weighted contrast agent at 3 T, and acting as a highly efficient T_2 weighted MRI contrast agent. **Figure 4A** shows the core-shell structure of prepared

NP-PAA-FA contrast agent, and the obtained high values of ratio r_2/r_1 at ultra-high-field indicate its ability for MRI contrast agent (**Figure 4B**). To confirm the dual-modal character of NP-PAA-FA contrast agent for MRI, phantom images of concentration dependent of NP-PAA-FA water solution are compared to that commercially available Dotarem or Fe_3O_4 contrast agent, showing the pronounced alterable contrast in both T_1 and T_2 images as a function of concentration (**Figure 4C**). Therefore, great potential of NP-PAA-FA as a multimodal constant agent has been demonstrated, which will pave the way for studying more, novel and suitable contrast agent for ultra-high-field MRI.

Despite the efficient of surface modification technique to improve the biocompatibility, nanobiointerface in conjunction with surface structure engineering provides another possibility to develop high performance dual-modal MRI contrast agent (Zhou et al., 2015a). Small molecules of sodium citrate and zwitterionic dopamine sulfonate are individually exploited as surface and interface modifier to realize the superior water-dispersibility. The surface chemical exchange has been carried out through a ligand exchange process via hydrothermal technique. The exposed iron and gadolinium ions of GdIOPs surface in promoting the T_1 relaxation are illustrated in **Figure 5A**, which is attributed to the efficient chemical exchange for protons provided by the
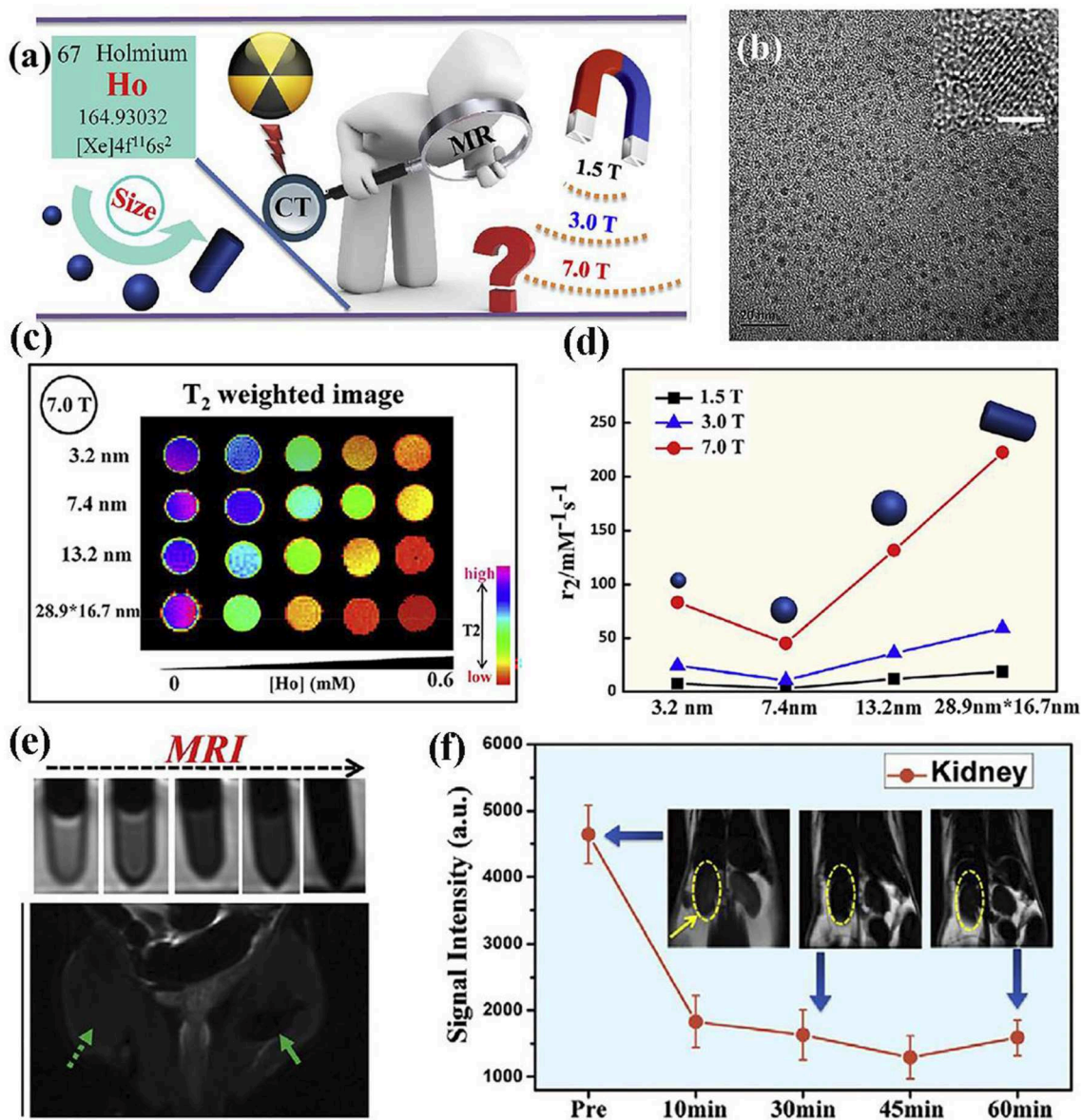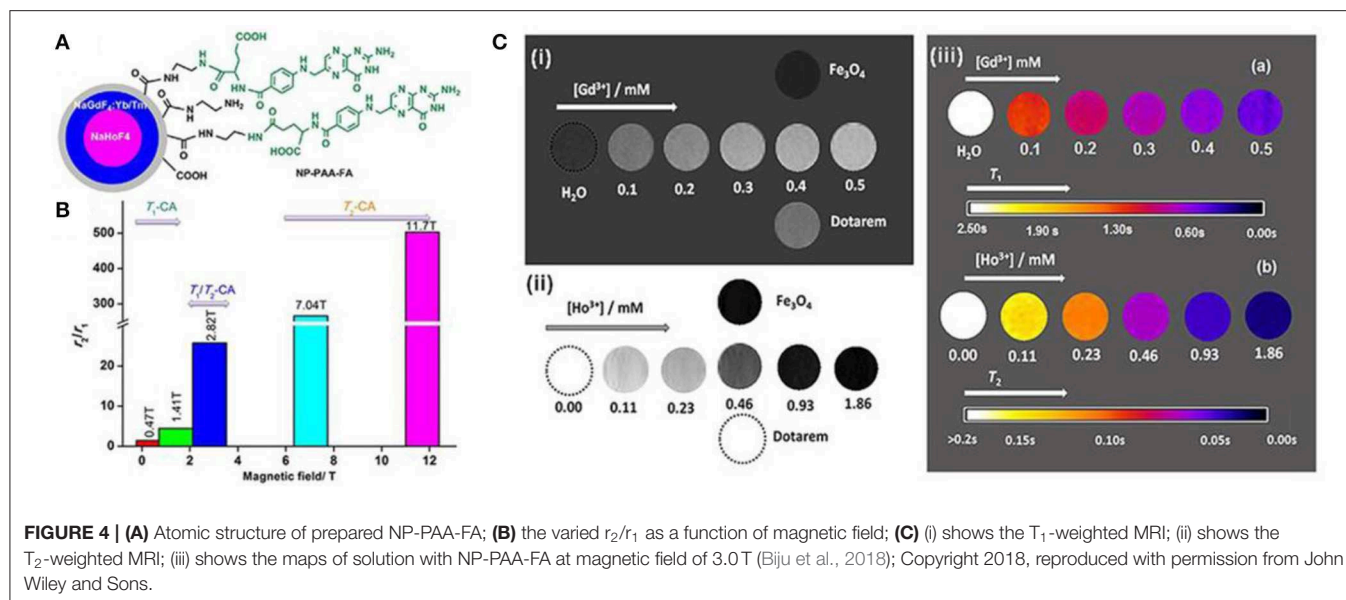
FIGURE 3 | (a) Schematic diagram of nanoparticle for high field MRI; **(b)** TEM image of nanoparticle (The scale bar of inset image is 2 nm); **(c)** nanoparticles with varied size at 7.0 T; **(d)** transverse relaxivity r_2 of nanoparticles with varied size at magnetic fields of 1.5, 3.0, and 7.0 T, respectively; **(e)** MRI of nanoparticles at different contents; **(f)** in vivo ultra-high-field MRI of kidney form mice after the intravenous injection of nanoparticles (Ni et al., 2016); Copyright 2016, reproduced with permission from Elsevier.

surface exposed ions (Zhou et al., 2015b; Shen et al., 2018). *In vivo* MRI performance has been performed at an ultra-high-field of 7.0 T to confirm the efficacy of dual-modal contrast agent served for liver imaging. **Figures 5B–E** show GdIOPs acting as T_1-T_2 dual-modal MRI contrast agent at an ultra-high-field of 7.0 T. MRI T_1 and T_2 images have been acquired at the targeted liver, showing both coronal and transverse plane images of liver at preinjection and each certain time postinjection. After 20 min injection, a rapid accumulation of contrast agent nanoparticles is reflected by the brighter contrast in T_1 imaging and a darker contrast in T_2 imaging results. Signal

to noise ratio changes (ΔSNR) reach to the maximum value for both T_1 and T_2 images at 60 min. Subsequently, the values rapidly drop at 240 min. This demonstrates the good metabolism of nanoparticle contrast agent in liver. Consequently, this kind of nanoparticles achieved through surface and interfacial engineering demonstrates its great promising as an ultra-high-field dual-modal MRI contrast agent for accurate diagnosis (Zheng et al., 2016; Kim et al., 2017). Moreover, recent advances of the relaxivity of nanoparticle contrast agents are summarized in **Table 1**, showing the great potential for ultra-high-field MRI.

FIGURE 4 | (A) Atomic structure of prepared NP-PAA-FA; **(B)** the varied r_2/r_1 as a function of magnetic field; **(C)** (i) shows the T_1-weighted MRI; (ii) shows the T_2-weighted MRI; (iii) shows the maps of solution with NP-PAA-FA at magnetic field of 3.0 T (Biju et al., 2018); Copyright 2018, reproduced with permission from John Wiley and Sons.

BIORESPONSIVE NANO-PLATFORMS MRI-BASED MULTIMODAL MOLECULAR IMAGING

Multimodal imaging is also highly desired to provide complementary information to improve the diagnosis accuracy (Sosnovik et al., 2007; Lee et al., 2012; Li et al., 2016, 2017; Anwaier et al., 2017; Kim et al., 2017). With the emerging the ultra-high-field T_2 MRI, molecular imaging capable of performing the characterization and measurement of biological process at cellular and molecular levels is highly demonstrated *in vivo* (Shin et al., 2015; Li and Meade, 2019). To realize molecular imaging, specific contrast agent and high sensitive instrument are both required to fulfill the scans with high resolution under high magnetic field (Chen et al., 2014). A variety of MRI contrast agents have been developed till now, which are non-specific contrast agent lacking the ability to reach specific target, targeted contrast agent, smart contrast agent, and the final labeled cells, respectively (Kim et al., 2017; Chang et al., 2020).

Multimodal molecular imaging is tremendously desired in recent years because of the limited resolution and inadequate information provided by each imaging modality. To achieve the high sensitivity and quantitative analysis in clinical diagnosis, multiple imaging modalities with nanoparticle contrast agents can be integrated to make up the complementary information. For instance, MRI possesses the advantages of relative high resolution ($25 \sim 100 \mu m$) and superior tissue penetration depth, while its sensitivity requires substantial improvement compared with the direct optical imaging technique. CT has the benefits of high resolution ($30 \sim 400 \mu m$) and 3D visual graphing; however, the low sensitivity also becomes the obstacle for its further wide application. Near-infrared fluorescence (NIRF) imaging share the benefit of high sensitivity, while it is constricted by the low spatial resolution. Computed tomography (CT) and MRI can provide the unparalleled structural information, while CT

and positron emission tomography (PET) can offer provide the insight into exploring the morphological and functional behaviors. Moreover, other combinations of multimodalities have been also attempted to resolve different upcoming issues in clinics., such as PET/MRI system into the dynamics of brain (Cho et al., 2008, 2013), MRI and CT (Ni et al., 2016), MRI and optical imaging to explore the evolution from single molecule to nanostructures (Harris et al., 2019), triple-modal imaging of NIRF/CT/MRI (Pansare et al., 2012; Hu et al., 2013; Liu et al., 2020), and dual-modality of MRI and single-photon emission computed tomography (SPECT), etc., (Dong et al., 2017; Li et al., 2019).

Figure 6A shows the schematic procedures of preparing hybrid nanoparticles. This kind of nanoparticles are used in tumor tissues to perform the diagnosis. The triple-modal NIRF/CT/MRI imaging results demonstrate the efficacy of nanoparticle contrast agent, showing the accuracy of targeting, low body residues. Interestingly, when the content is lowered to $2.1 \mu M$, contrasted signals of NIRF/CT/MRI can be revealed by the contrast agent (**Figure 6B**). Therefore, the synergistic effect of NIRF/CT/MRI triple-modal imaging has been indicated, showing the complementary information of structural and functional imaging for tumor tissue (Hu et al., 2013). In addition, dual-modality of MRI and SPECT imaging has been endeavored to assist the detection of gene reporters to track viable cells *in vivo*. **Figures 6C,D** shows the individual MRI image and SPECT image after injecting each specific contrast agent. When MRI and SPECT are integrated for diagnosis, the combined image of dual-modality is shown in **Figure 6E**, which paves the way for further investigation of cells and gene patterns in gene expression with the multimodal molecular imaging technique (Jung et al., 2020; Song et al., 2020).

On the other hand, nanoparticle functionalization in contrast agent is playing a significant role in monitoring and revealing
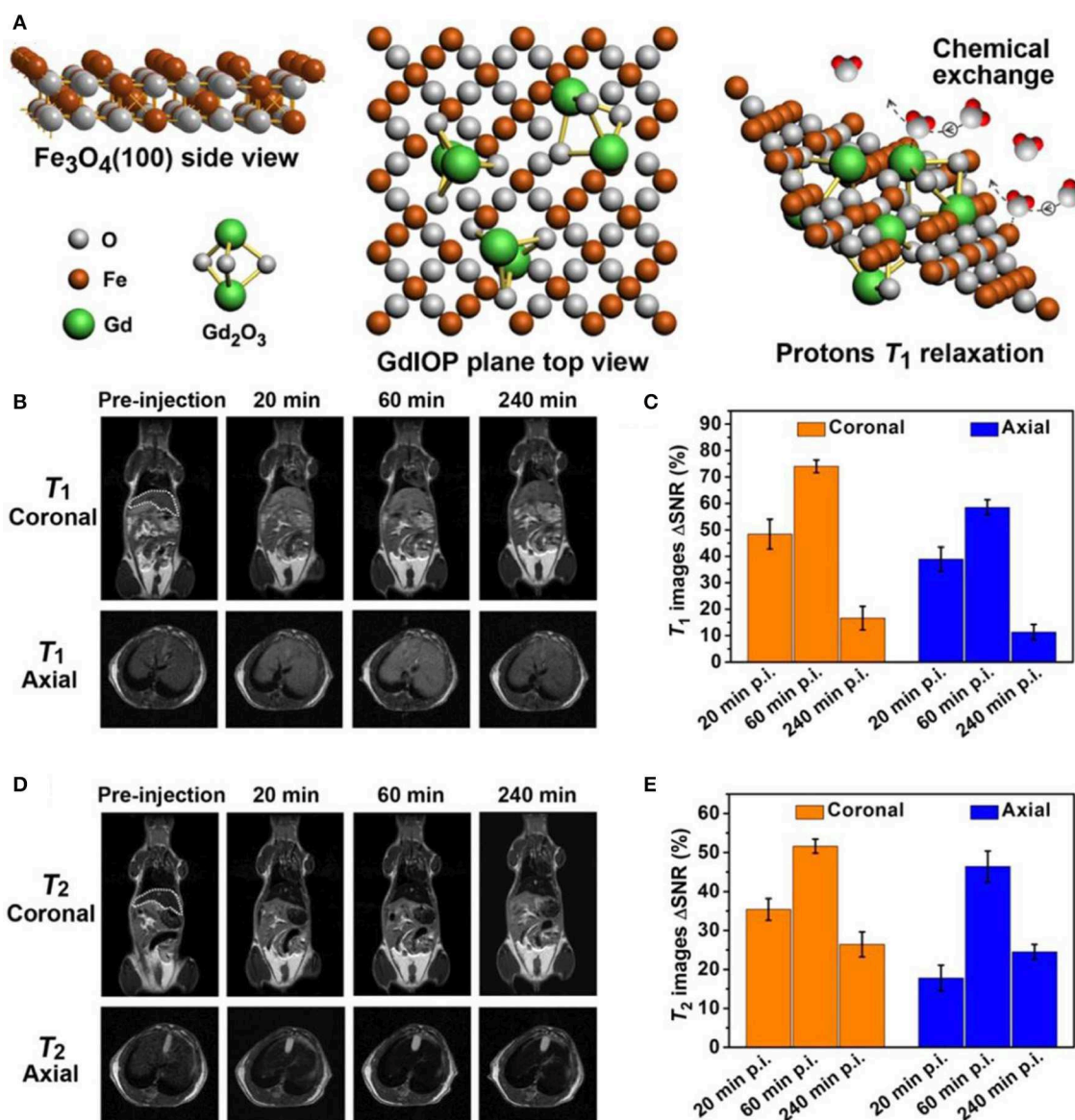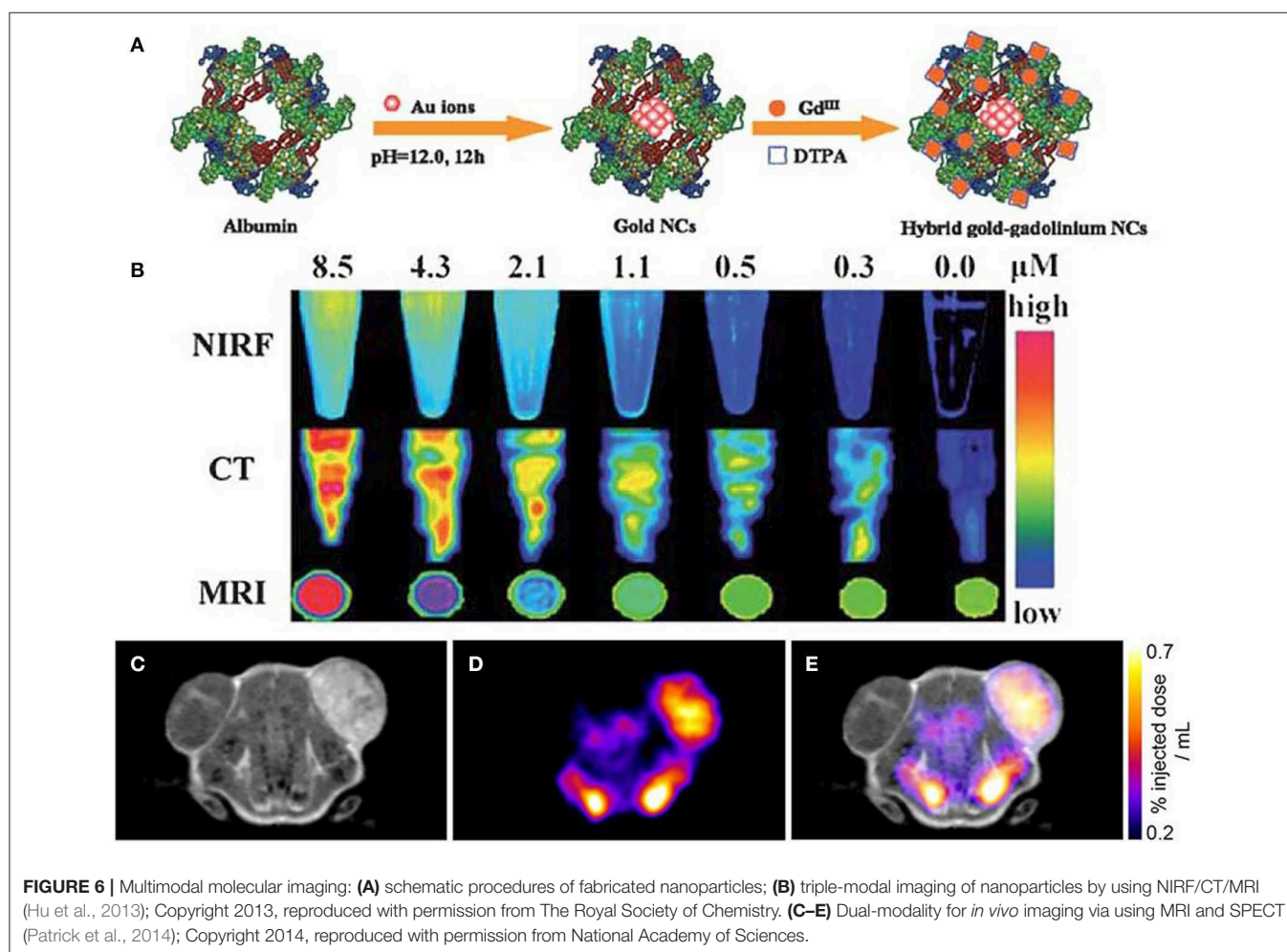
FIGURE 5 | T_1-T_2 dual-modal MRI at ultra-high-field of 7.0 T: **(A)** Atomic structure of GdIOPs, including the top view of Fe_3O_4, plane to view of GdIOP and chemical exchange in promoting protons T_1 relaxation. **(B–E)** GdIOPs acting as T_1-T_2 dual-modal MRI contrast agents (Zhou et al., 2015a); Copyright 2015, reproduced with permission from American Chemical Society.

the diagnosis information at the molecule level, which is accomplished through the combination of dual-modality or tri-modality imaging. Nanoparticle functionalization is performed via indirect or direct surface modification of nanoparticles, where folic acid, oligo nucleotides and peptides, etc., can be exploited as the surfactants (Zhou et al., 2012; Huang et al., 2015; Gao et al., 2017; Thiruppathi et al., 2017). After the functionalization of nanoparticles, these contrast agents are embraced with the advantages of good physical properties, non-invasive, well-dispersed, and homogenous, eventually to achieve the improved efficiency, and abundant modality.
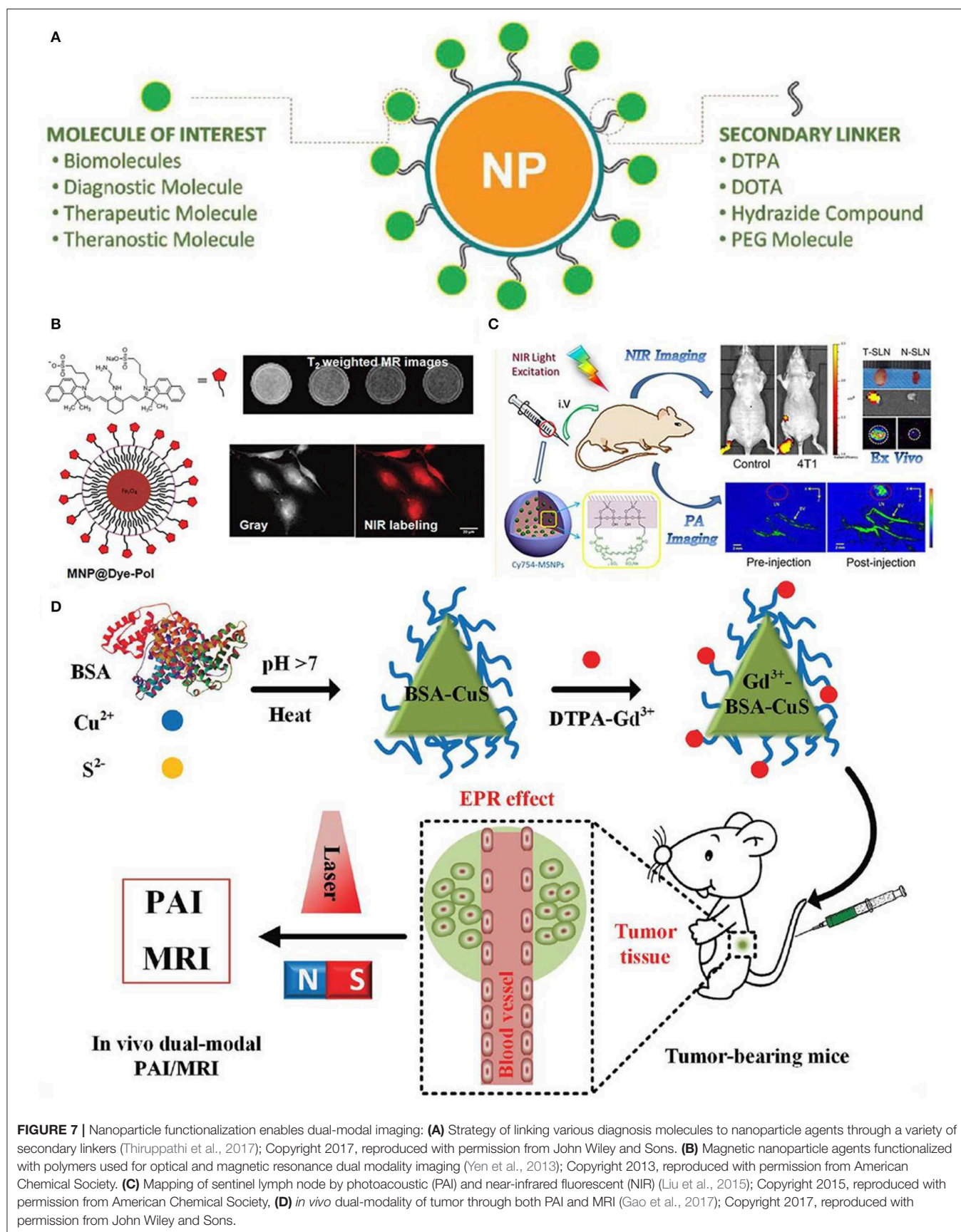
Figure 7A shows the functionalized nanoparticles capable of dual-modal imaging, where strategy of linking various diagnosis molecules to nanoparticle contrast agents is illustrated through a variety of secondary linkers (Thiruppathi et al., 2017). To further verify this kind of developed strategy, magnetic nanoparticles are specifically functionalized with polymer linkers and then NIR dye for optical and magnetic resonance imaging (**Figure 7B**), demonstrating the efficacy of using functionalized nanoparticles for multi-modal imaging (Yen et al., 2013). Moreover, nanoparticles modified with two ligands demonstrate the enhanced targeting efficiency and promote the better clearing of tumor growth at large level, which are ascribed to the

TABLE 1 | Comparison of the relaxivity of bioresponsive nano-sized contrast agents for ultra-high-field MRI.

Nanoparticles	Size (nm)	Magnetic field (T)	r_1 (mM^{-1}s^{-1})	r_2 (mM^{-1}s^{-1})	r_2/r_1	References
DEG-Gd$_2$O$_3$	4.6	7.0	4.4	28.9	6.6	Bridot et al., 2007
PEG-Gd$_2$O$_3$	1.3	11.7	10.4	17.2	1.65	Faucher et al., 2012
MnFe$_2$O$_4$	7.6	9.4	18.6	227.6	12.2	Kim et al., 2009
CoFe$_2$O$_4$	8.0	9.4	6.3	392.5	62.3	Kim et al., 2009
PEG-ZnFe$_2$O$_4$	5.9	9.4	0.60	49	82	Banerjee et al., 2017
Fe$_3$O$_4$	20	7.0		679		Zhao et al., 2013
Dy$_2$O$_3$	60/70	17.6/7.0		675/190		Norek et al., 2008
Fe$_3$O$_4$ sphere	65	7.0		249		Huang et al., 2010
Fe$_3$O$_4$ brick-like	64.0	7.0	4.3	599	139	Worden et al., 2015
NaDyF$_4$ sphere	20.3	9.4		101		Das et al., 2012
PMAO-PEG/ NaDyF$_4$	25×35	9.4	0.50	204.4	410	Zhang et al., 2016
NaHoF$_4$	13.2	7.0	0.35	131.7	376	Ni et al., 2016
PMAO-PEG/NaHoF$_4$	17	9.4	0.17	130.6	768	Zhang et al., 2016
QD-CAAKA-DOTA-Dy	5.5	21.1	0.08	57.4	718	Rosenberg et al., 2010
GdIOPs	12	7.0/9.4	6.8/4.3	158.8/167.6	23.4/38.9	Zhou et al., 2015a
NP-PAA-FA	24	7.04/11.7	0.32/0.29	85/146	266/503	Biju et al., 2018

FIGURE 6 | Multimodal molecular imaging: **(A)** schematic procedures of fabricated nanoparticles; **(B)** triple-modal imaging of nanoparticles by using NIRF/CT/MRI (Hu et al., 2013); Copyright 2013, reproduced with permission from The Royal Society of Chemistry. **(C–E)** Dual-modality for *in vivo* imaging via using MRI and SPECT (Patrick et al., 2014); Copyright 2014, reproduced with permission from National Academy of Sciences.

FIGURE 7 | Nanoparticle functionalization enables dual-modal imaging: (A) Strategy of linking various diagnosis molecules to nanoparticle agents through a variety of secondary linkers (Thiruppathi et al., 2017); Copyright 2017, reproduced with permission from John Wiley and Sons. (B) Magnetic nanoparticle agents functionalized with polymers used for optical and magnetic resonance dual modality imaging (Yen et al., 2013); Copyright 2013, reproduced with permission from American Chemical Society. (C) Mapping of sentinel lymph node by photoacoustic (PAI) and near-infrared fluorescent (NIR) (Liu et al., 2015); Copyright 2015, reproduced with permission from American Chemical Society, (D) in vivo dual-modality of tumor through both PAI and MRI (Gao et al., 2017); Copyright 2017, reproduced with permission from John Wiley and Sons.

enormously increasing uptake of functionalized nanoparticle contrast agents.

In addition, **Figure 7C** shows the mapping of sentinel lymph node by dual-modality of photoacoustic (PAI) and near-infrared fluorescent (NIR), where fluorescent dye-loaded mesoporous silica nanoparticles imaging contrast are employed to study the tumor metastasis model as well as the underlying molecular level mechanism of dual-modality imaging (Liu et al., 2015). As shown in **Figure 7C**, surface functionalized nanoparticles in conjunction with dual-modality imaging are used to visualize sentinel lymph nodes up to 2 weeks based on the tumor metastatic model. Moreover, differences of uptake rate and contrast between normal sentinel lymph nodes and metastasized sentinel lymph nodes are compared, showing the feasibility of functionalized nanoparticles in identifying tumor metastasis based on dual-modality imaging results.

Interestingly, water-soluble functionalized nanoparticle contrast agent has been showing its great significance in detecting cancer at early stage. For instance, **Figure 7D** shows the protein-modified hydrophilic copper sulfide (CuS) used as dual-modality nanoprobe, which opens a new avenue for both photoacoustic imaging and MRI in cancer diagnosis (Gao et al., 2017). This kind of functionalized nanoparticles possess the following advantages: good biocompatible and water-soluble, controllable small size with good stability, feasibly functionalized (Gao et al., 2018). *In vivo* test has been conducted in a subcutaneous tumor mouse with this functionalized nanoparticle contrast agents, showing the improved accuracy in both resolution and contrast. Therefore, with the unique properties of this protein-modified nanostructures, nanoplatform aiming for dual-modality imaging can be designed to target disease diagnosis.

Except for dual-modality imaging, the tri-modality imaging with functionalized nanoparticles has also been endeavored by researchers. Surface-enhanced Raman spectroscopy (SERS) is proposed as a sensitive and non-invasive technique, which provides precise and specific identification of signals in combination with nanoparticle contrast agents. Iterative coating approach is used to reach the rational design and synthesis of core/shell magnetic nanoflower contrast agent (Huang et al., 2015). Thus, remarkable SERS enhancement, superior PA signals, improved relaxivity, and the effective photothermal effect are achieved with this contrast agent. The combination of MRI/PA/SERS techniques has been put forward to achieve the synergistic tri-modality imaging, where MRI is responsible for the contour and localization of tumor diagnosis, PA for deep localizaiton and anatomical and SERS is for margin identification (**Figure 8A**. In addition, functional biomarker of water-soluble melanin nanoparticle is to target for melanoma imaging (**Figure 8B**). After conjugating surfactants of $\alpha_v\beta_3$ integrins and cyclic peptide to melanin nanoparticle, the U87MG tumor accumulation is observed owing to the synergistic effect of enhanced permeability and retention (Fan et al., 2014). With the combinations of different modalities of PET/MRI/PAI techniques, it is anticipated to provide guidance for localizing both superficial and deep tumor surgery. As a result, this kind of water-soluble melanin nanoparticle contrast agent after biomolecules modification shows the tremendous feasibility in

multimodal imaging and can be also used as nanoplatform for potential therapeutic applications.

Therefore, through the proof-of-concept design in functionalized nanoparticle contrast agents, a general and versatile strategy can be developed to realize the multimodal imaging with functional molecular probes.

TARGETED MOLECULAR IMAGING AGENTS

Targeted molecular imaging agents in combination with imaging probe are proposed to non-invasively identify cellular processes in varied stages of disease, which generally include metabolic targeted, anti-body targeted, peptide, and activity-based probes (Zhao et al., 2012; Galluzzi et al., 2013; Chen et al., 2014; Craig et al., 2016; Dearling et al., 2016; Lee et al., 2016; Zhang et al., 2017; Mulder et al., 2018; Dammes and Peer, 2020). Peptide shows the advantages of good selectivity and specificity, which belongs to a class of ligand used for MRI (Lee et al., 2010; Craig et al., 2016). Moreover, with the surface modification of targeted molecular imaging agents, the pronounced improvement of targeting efficacy is achieved compared to that of anti-body agents, which is attributed to the controlled size of agent and its large number of ligands (Cai and Chen, 2007). To be eventually exploited as the desired targeted molecular imaging agents, a number of crucial factors need to be considered based on the agent-specific basis principle, such as the toxicity, extent of resection (EOR), the efficient and efficacy of delivery to target issue and the induced side effect. With the targeted imaging agents and probes, studies covering from imaging of breast cancer, cardiovascular disease and neurodegenerative disease has been conducted. However, much remains to be resolved before the practical *in vivo* applications, which includes the aspects of *in vivo* kinetics, efficacy, diagnostic accuracy and sensitivity, biocompatibility, chronic toxicity and the cost.
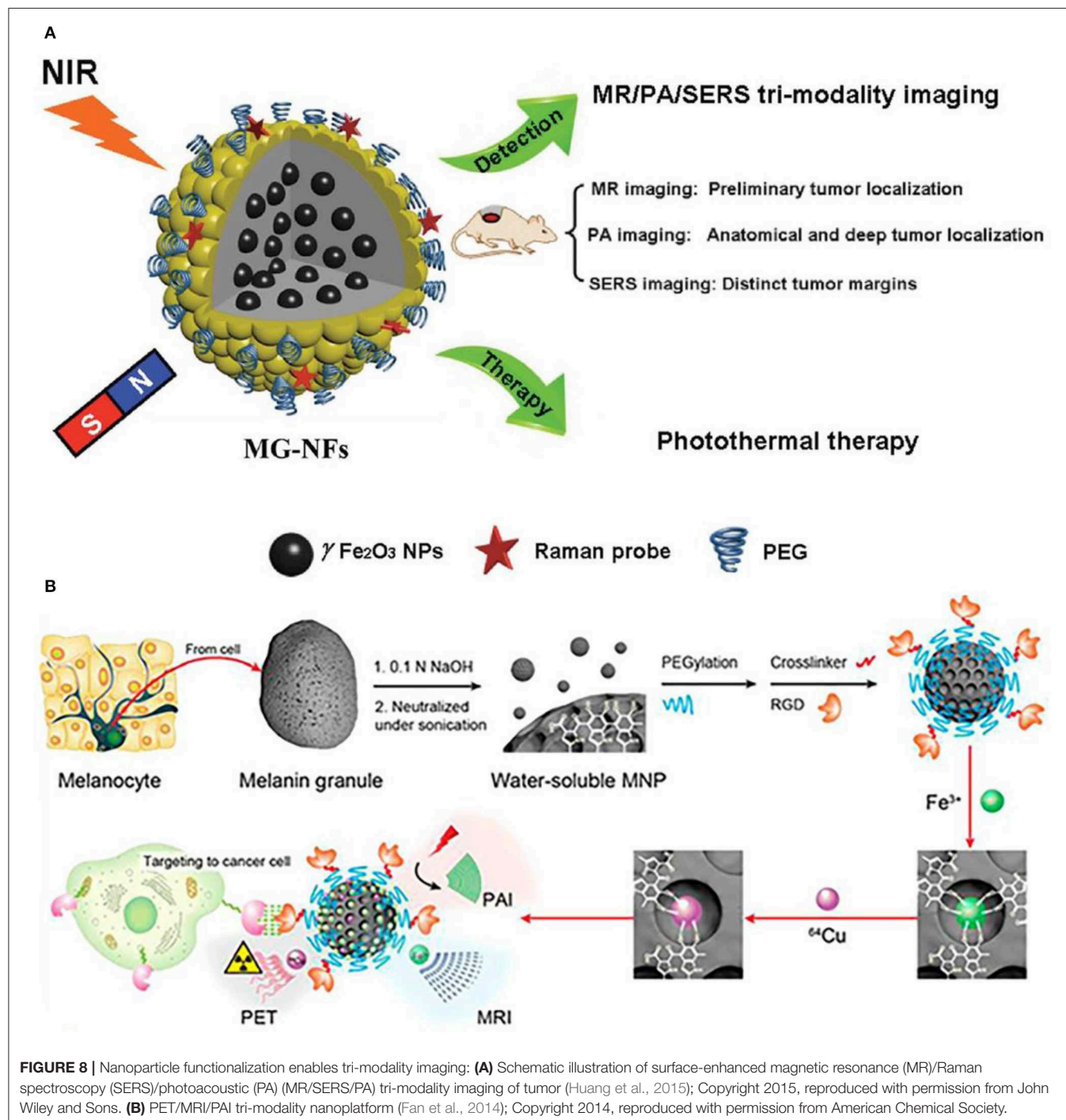
To predict and assess the metabolic alternation in tumor tissues, a non-invasive quantitative MRI approach has been exploited, where the Dixon-based MRI acts as the biomarker to predict the tumor aggressiveness before surgical intervention. **Figure 9A** shows the metabolic targeted molecular imaging agents, where tissue-based analysis has been performed with MRI quantitative parameters in anatomical coregistration. After undergoing MRI for patients, the Dixon-based MRI-derived quantitative analysis for *in vivo* fat quantification can be proceeded, showing the role of *in vivo* biomarker of metabolic targeted agents in clear cell renal carcinoma (ccRCC) (Zhang et al., 2017). To evaluate the efficacy of anti-body targeted agents, research work has been conducted to detect the colitis in a mouse model via using the imaging probe. The FIB504.64 shows a pronounced specific uptake, which is revealed by the evident observed colitis (**Figure 9B**), showing its capability as a promising disease-specific imaging agent (Dearling et al., 2016).

A variety of peptide receptors capable of targeting tumor tissues are reported in molecular biology, such as $\alpha_v\beta_3$, glucagon-like peptide-1, somatostatin and gastrin-releasing peptide. The
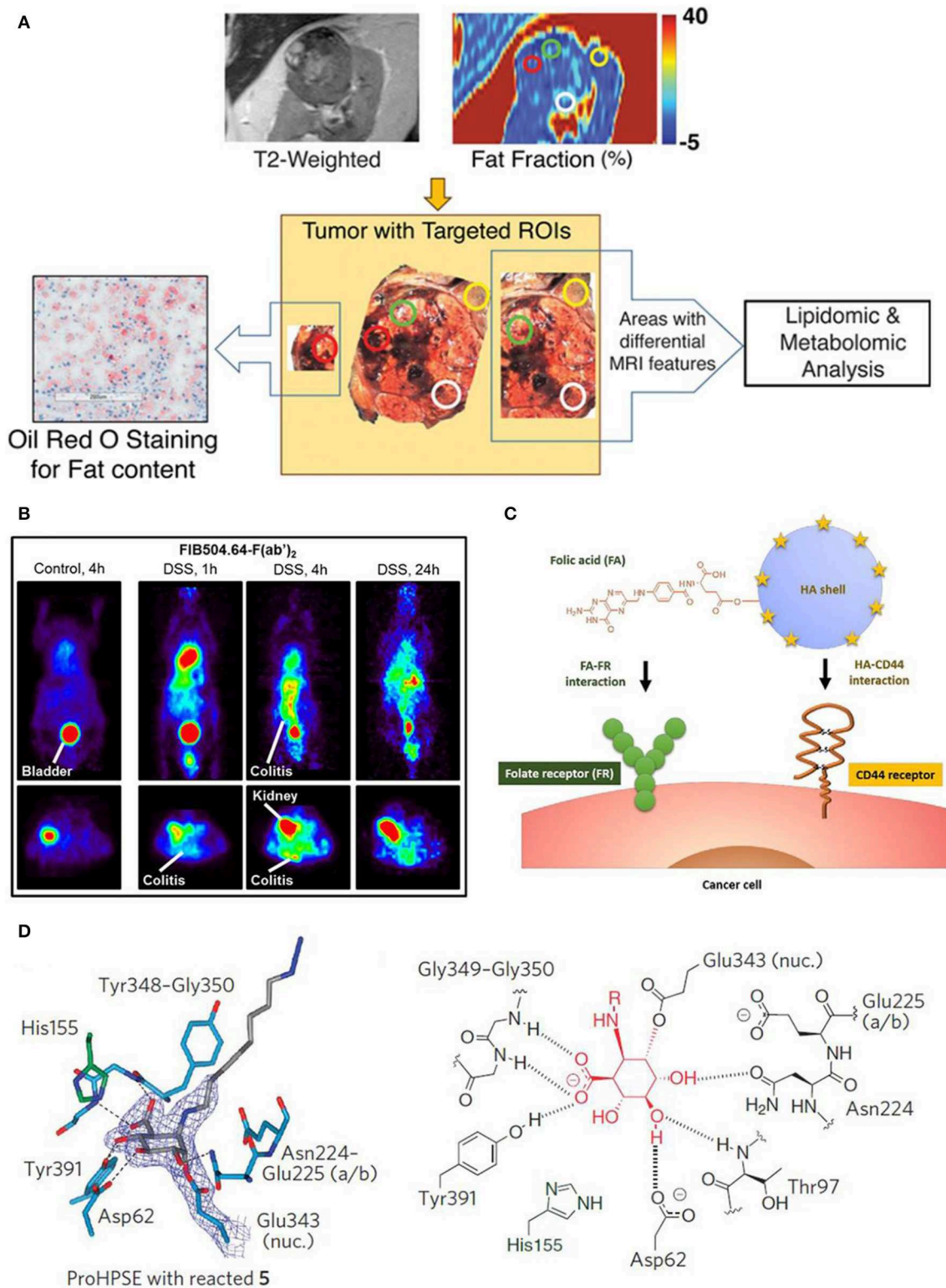
strategy of integrating multiple ligands into tumor tissues has been adopted to harvest more potential binding sites and *in vivo* ultrasound intensity. For instance, hyaluronic acid ceramide folic acid nanoparticles (HACE-FA NPs) are reported to target both CD44 and folate receptor (FR) (**Figure 9C**), showing their synergistic effect to increase affinity of agents to receptors (Lee et al., 2016; Ko et al., 2019). Moreover, to achieve the specific diseased sites imaging, monoclonal antibodies are

prevalently used owing to their merits of specificity, affinity and serum stability.

Given the significance of β-glycosidases in human body, a set of β-glycosidase-specific activity-based probes (ABPs) are specifically studied to detect enzymatic activity over a range of glycosidases, demonstrating its role of tracking pathological relevant enzymes and its great potential in discovering the structural and biochemical

FIGURE 8 | Nanoparticle functionalization enables tri-modality imaging: **(A)** Schematic illustration of surface-enhanced magnetic resonance (MR)/Raman spectroscopy (SERS)/photoacoustic (PA) (MR/SERS/PA) tri-modality imaging of tumor (Huang et al., 2015); Copyright 2015, reproduced with permission from John Wiley and Sons. **(B)** PET/MRI/PAI tri-modality nanoplatform (Fan et al., 2014); Copyright 2014, reproduced with permission from American Chemical Society.

FIGURE 9 | Targeted molecular imaging agents: **(A)** Metabolic targeted agents to proceed the tissue-based analysis with MRI quantitative parameters in anatomical coregistration (Zhang et al., 2017); Copyright 2017, reproduced with permission from Clinical Medicine. **(B)** Anti-body targeted agents (Dearling et al., 2016); Copyright 2016, reproduced with permission from Crohn's & Colitis Foundation of America. **(C)** Schematic diagram of peptide targeted HACE-FA NPs to tumor tissues (Lee et al., 2016); Copyright 2016, reproduced with permission from Elsevier. **(D)** Activity based targeted agents (Zhao et al., 2012); Copyright 2017, reproduced with permission from Nature Chemical Biology.

functionality (Wu et al., 2017). **Figure 7D** shows the active site interaction with ABPs, where hydrogen bonding interactions identical to that of mature enzyme are illustrated in **Figure 9D**. Therefore, this activity based targeted agent offers a powerful tool in characterizing enzyme activities.
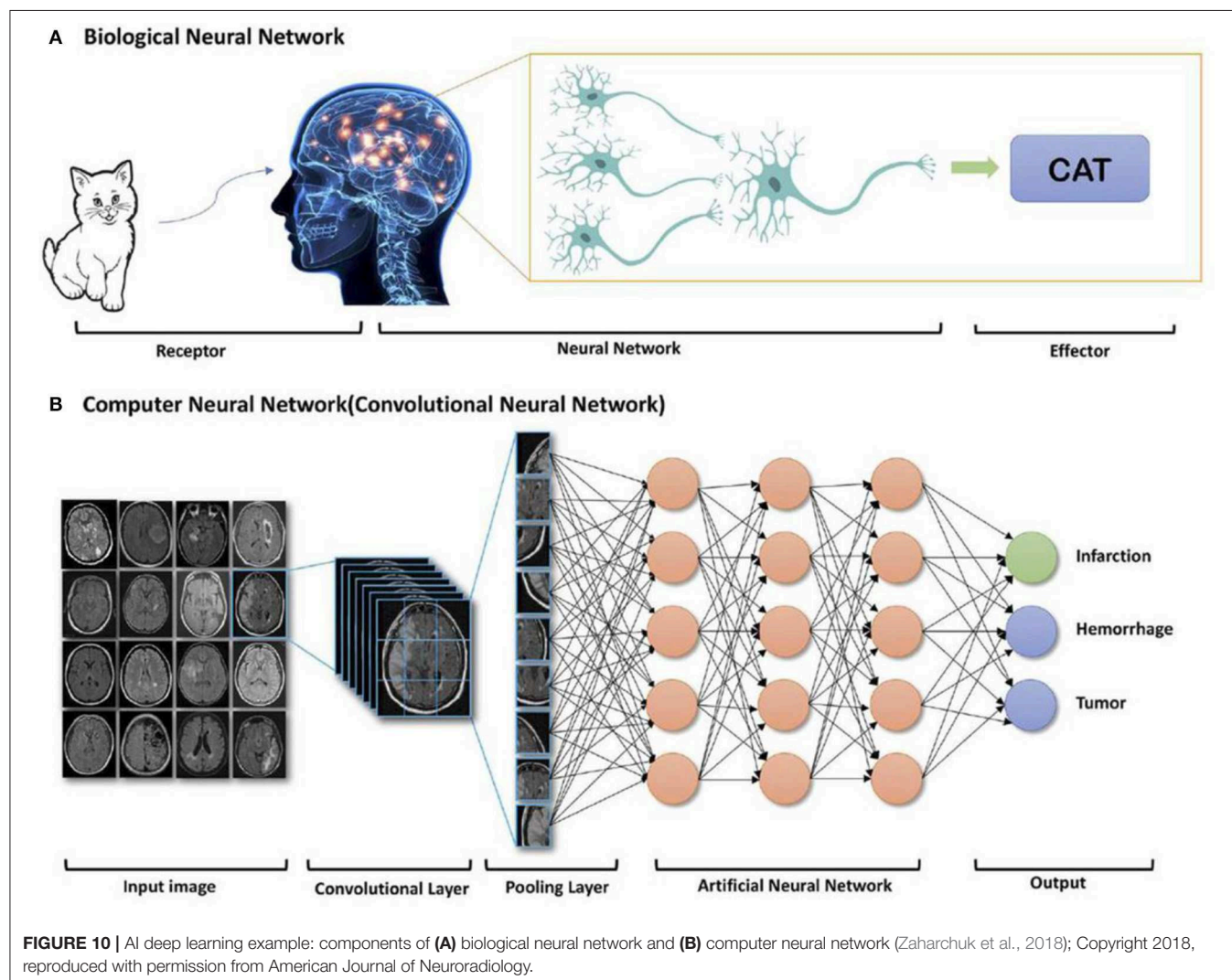
Upon further improvement of target molecular imaging agents for ultra-high-field MRI, specific molecular therapy with tremendously enhanced accuracy and sensitivity will profoundly impact future clinical diagnosis.

THE ROLE OF ARTIFICIAL INTELLIGENCE FOR DEVELOPING NOVEL/BIORESPONSIVE NANO AGENTS FOR MRI

One of the innovative clinical applications of AI lies in medical imaging, which includes the following aspects: image acquisition,

removing the unwanted artifacts, improving the image quality, reducing the contrast agent dose, and shortening the diagnose period (Gong et al., 2018; Shan et al., 2018; Zaharchuk et al., 2018; Codari et al., 2019; Zhu et al., 2019).

For biomedical imaging, the image reconstruction can be improved by exploiting machine learning or deep learning of AI, where powerful graphical processing units and neural networks formed in computer will assist the reconstruction processing (Gong et al., 2018; Shan et al., 2018; Zaharchuk et al., 2018). Alternatively, after accessing to large amount of information, the deep learning of AI will be processed and form an algorithm based on these inputs. **Figure 10** shows the whole process of biological neural network, where receptor receives a cat as inputting information, after learning process, cat has been reconstructed at the effector side. Moreover, convolutional neural network is another type of learning method of AI, where the algorithm will be configured to proceed further analysis based on the previous inputs (Bernal et al., 2019). Therefore, deep

FIGURE 10 | AI deep learning example: components of **(A)** biological neural network and **(B)** computer neural network (Zaharchuk et al., 2018); Copyright 2018, reproduced with permission from American Journal of Neuroradiology.

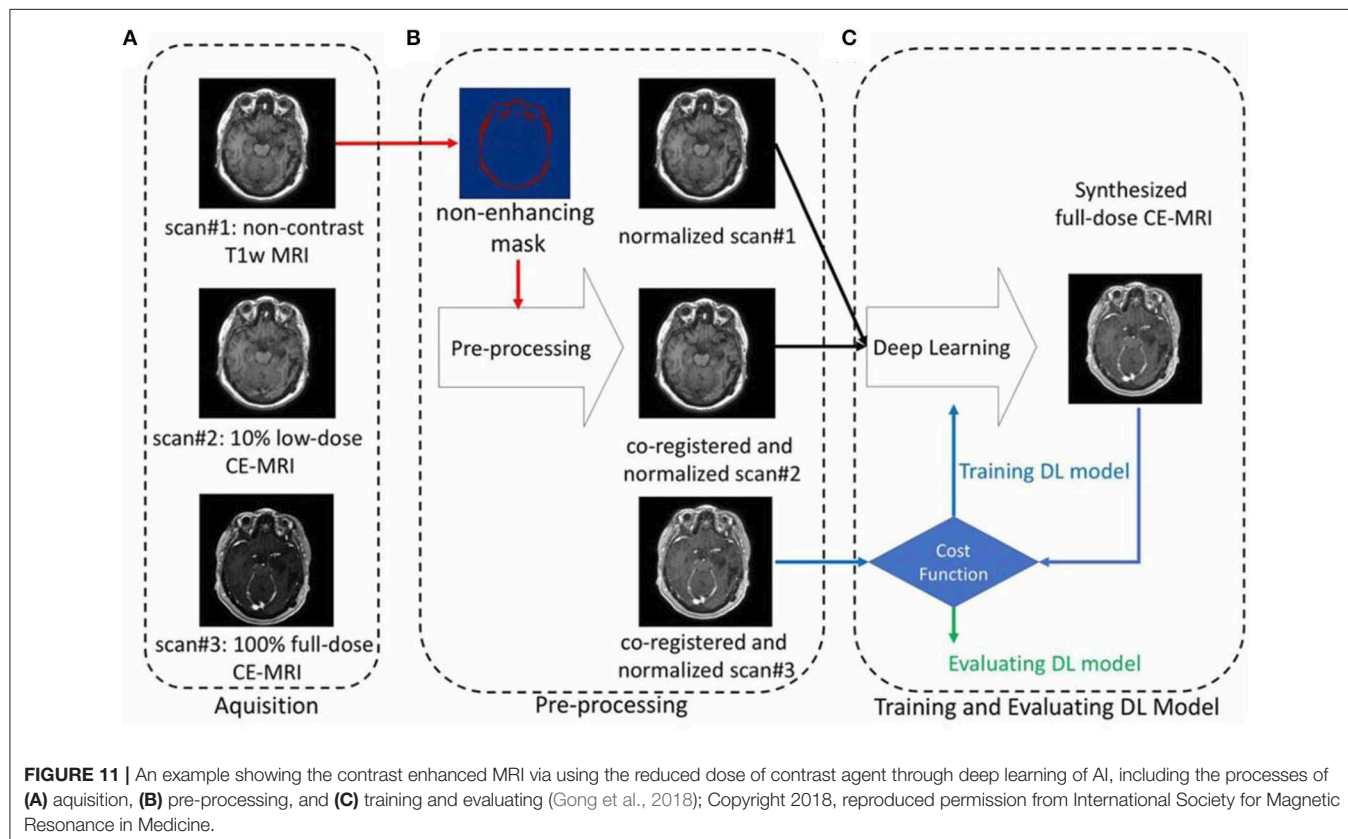learning of AI can assist MRI scans to acquire images with enhanced quality.

To maintain the diagnostic quality, it is also aimed to reduce the MRI contrast agent dose. As heavy metal gadolinium is indispensably used as MRI contrast agent and can remain in human body after scans, researchers are trying to improve the safety of patients after keeping the achieved scan information. Therefore, deep machine learning of AI can be implemented based on designed experiments, that is contrast agent experiment of less dose by comparing with that of no dose and full dose (Gong et al., 2018). For instance, Gong et al. performed an attempt on contrast enhanced MRI with low dose of contrast agent through deep learning of AI (**Figure 11**). By employing the non-contrast MRI and low-contrast MRI as inputs for deep learning, simulated model/algorithm will be predicted based on the obtained signal difference between non-contrast MRI and low-contrast MRI (Raval et al., 2017). Subsequently, this algorithm will be used to synthesize a full does contrast enhanced MRI to verify the formerly set-up full dose MRI. These results indicate that much useful clinical information can be obtained through using the enormously reduced dose of contrast agent based on the deep learning of AI.

On the other hand, the shortened diagnosis time is enormously expected in high field MRI with the aid of AI. To obtain a high or super-resolution MRI, ultra-high magnetic field (over 7 T) is generally required to perform the scan with contrast agent, which will inevita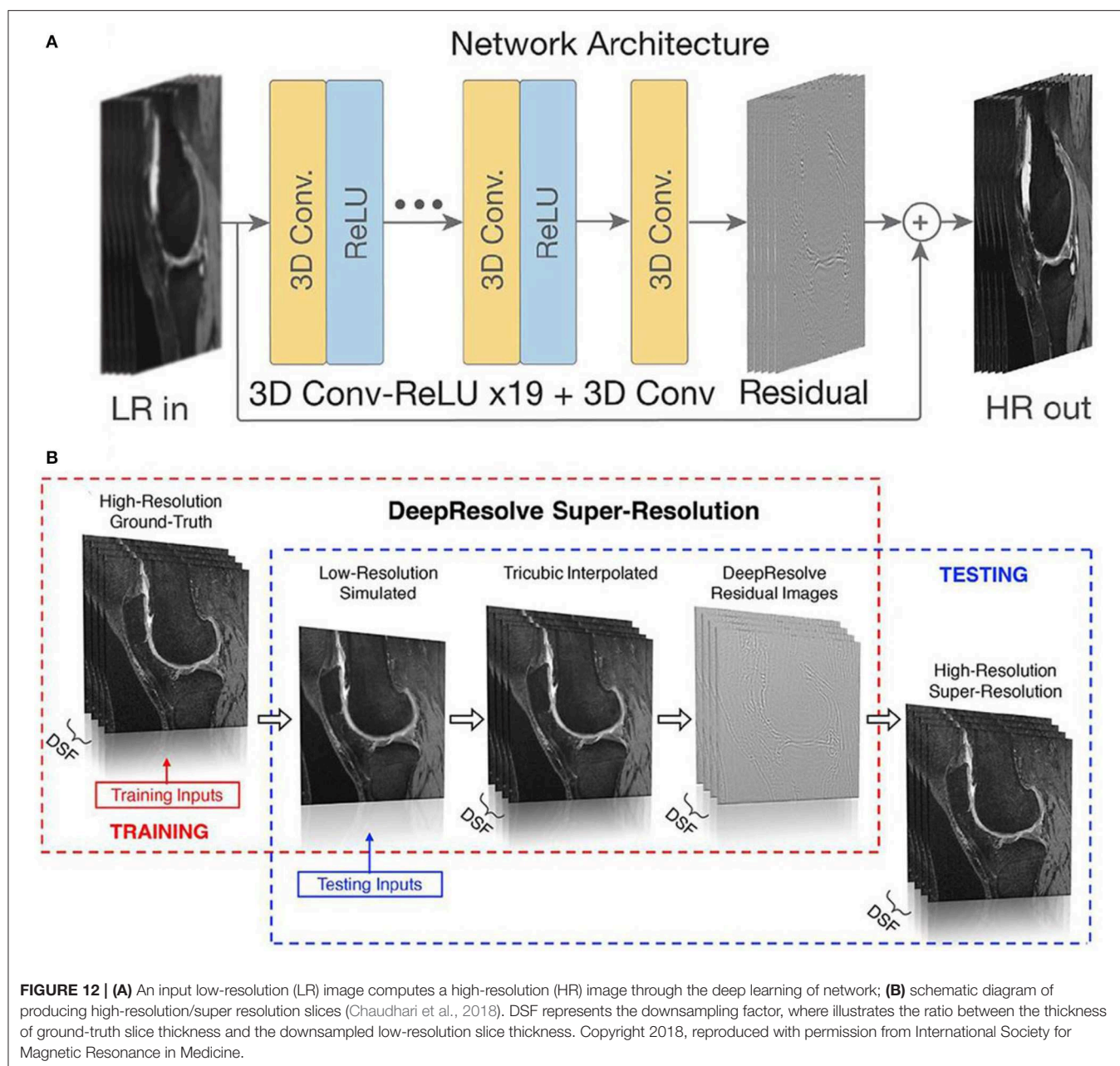bly induce high cost of equipment purchase and high operational cost of long-tern scanning, and the unexpected unsafety issue owing to the high magnetic field. Until now, many attempts have been devoted to exploiting machine learning of AI to replace the high field scan process, where high resolution MRI can be obtained through AI deep learning of low-resolution MRI (Shen et al., 2017a; Mahmud et al., 2018; Wegmayr et al., 2018; Mostapha and Styner, 2019; Nalepa et al., 2020). For instance, Chaudhari et al. developed a super-resolution approach to generate MRI information of thin-slice knee from thicker ones through the configured convolutional neural networks of AI deep learning (**Figure 12**) (Chaudhari et al., 2018). Furthermore, Lyu et al. adapted two latest neural network models to realize super-resolution MRI, showing a 2-fold enhancements of resolution in MRI (Lyu et al., 2018). Therefore, with the emerging of AI, it is promising to achieve high resolution MRI without the expensive high field instrument and long-term scanning.

PROSPECTS AND CHALLENGES

With the aim of developing contrast agents with good compatibility, biodegradability, high relaxivity for MRI and ultra-high-field MRI, continuous efforts have been devoted to exploring and searching for better contrast agents for MRI. To improve the imaging sensitivity of nanoparticle contrast agents, geometry of size, surface, shape of nanoparticles can be designed, and tuned via surface modification approaches, or other

FIGURE 11 | An example showing the contrast enhanced MRI via using the reduced dose of contrast agent through deep learning of AI, including the processes of **(A)** aquisition, **(B)** pre-processing, and **(C)** training and evaluating (Gong et al., 2018); Copyright 2018, reproduced permission from International Society for Magnetic Resonance in Medicine.

FIGURE 12 | (A) An input low-resolution (LR) image computes a high-resolution (HR) image through the deep learning of network; **(B)** schematic diagram of producing high-resolution/super resolution slices (Chaudhari et al., 2018). DSF represents the downsampling factor, where illustrates the ratio between the thickness of ground-truth slice thickness and the downsampled low-resolution slice thickness. Copyright 2018, reproduced with permission from International Society for Magnetic Resonance in Medicine.

techniques (Zhou et al., 2019). Cutting-edge interdisciplinary subjects of chemistry, physical, biological, and engineering shall also be included to resolve the current limitations of developing nanoparticle contrast agents. After implementing the rational design and surface modification of nanoparticles, this will inevitably promote MRI capable of molecular imaging for better monitoring during biological process (Zhu and Moser, 2017; Basal and Allen, 2018). For instance, **Figure 13** shows a representative example about the functionalized nanoparticle contrast agents ranging from the initial design to the final multimodal imaging applications, where doping technique has been adopted to functionalize a variety of nanoparticles with the employed various surfactants, such

as poly(allylamine hydrochloride) (PAH), polyacrylic acid, and polyethylene glycol (PEG). Meanwhile, nanoparticle contrast agents are not just limited to Fe^{2+}, Fe^{3+}, Mn^{2+} based nanoparticles (Zhu et al., 2015). Other bioresponsive nano-sized contrast agents used for high field magnetic resonance imaging can also be employed for the surface functionalization, eventually to act as the molecular probes for multimodal imaging of photoacoustic (PA) imaging and MRI imaging, etc. (He et al., 2018). Consequently, wide applications of high field MRI, multimodal imaging, and theragnostic technique into MRI will be also promoted by the synergistic effect of both molecular probes and a variety of imaging techniques.
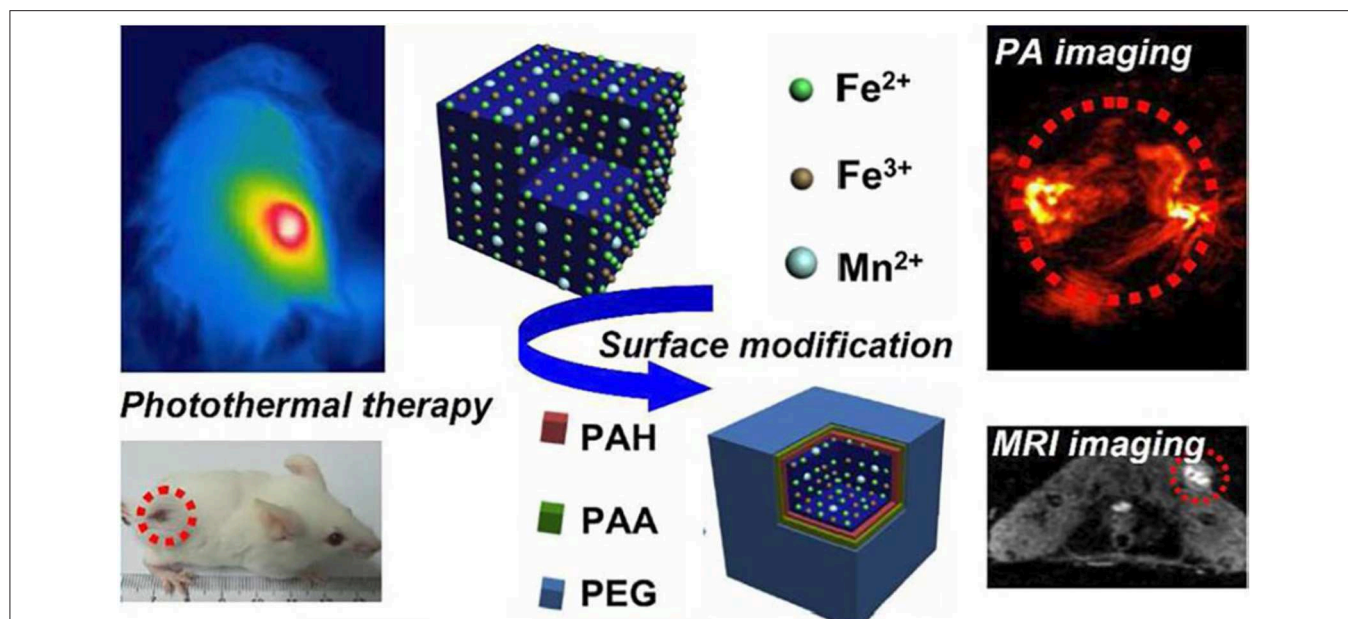
FIGURE 13 | Multimodal probes: from design to biology applications (Zhu et al., 2015); Copyright 2015, reproduced with permission from American Chemical Society.
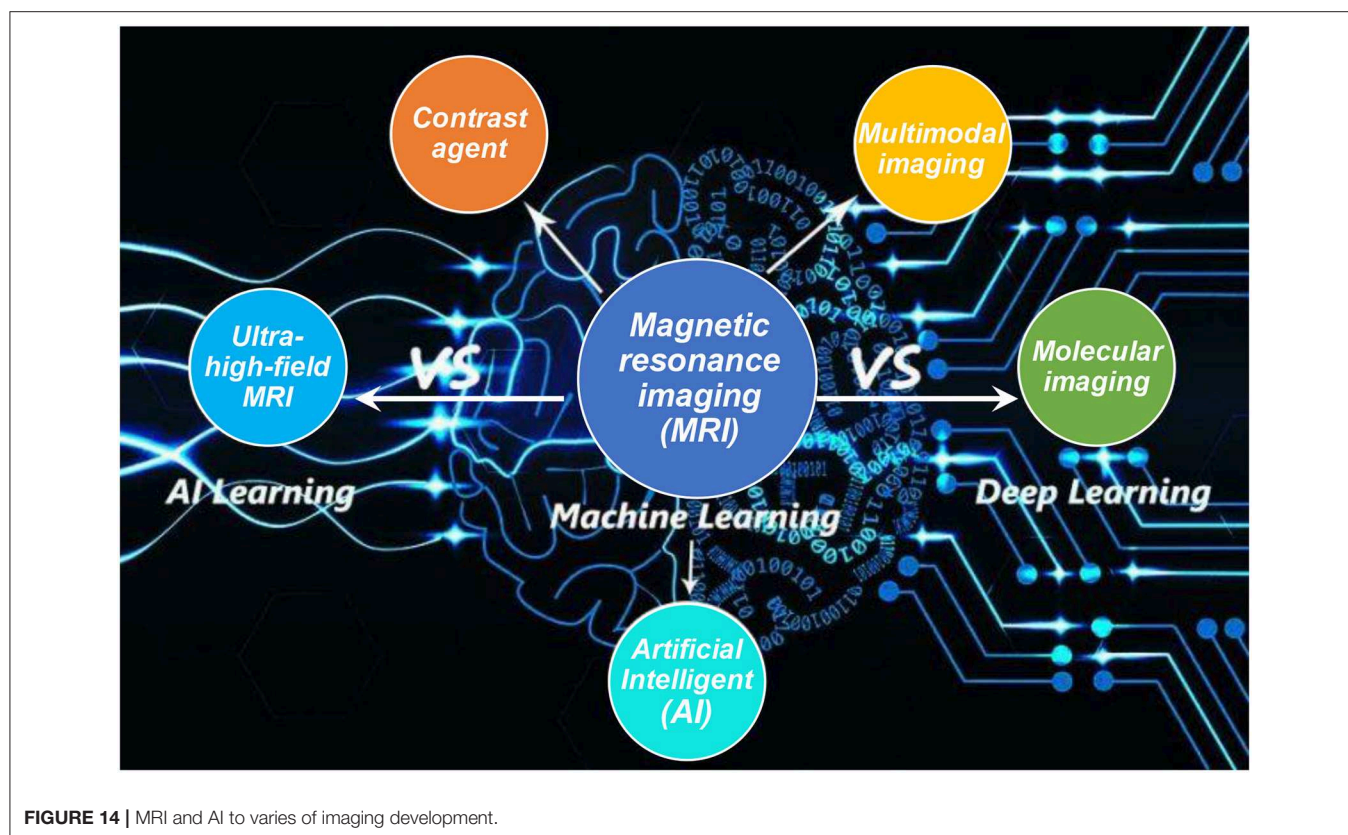

FIGURE 14 | MRI and AI to varies of imaging development.

In addition, based on the design principles of nanoparticle contrast agents, crucial aspects in terms of easy-processable and low cost are considered to meet the large-scale demands, which can be resolved with the assistance of AI technology.

As the fabrications of nanoparticle contrast agents focus on optimizing a variety of parameters, with the emerging of AI, the algorithm based on the deep learning will complete all these tasks prior to perform the final optimized experiments

for verification, which will save substantial time, efforts and achieve the high resolution MRI (Moser et al., 2017; Raval et al., 2017). Furthermore, for future MRI, it is suggested to employ the convolutional neural networks in AI deep learning to get the multimodal imaging information with high resolution (**Figure 14**), where the conventional MRI can only achieve single information with the applied high magnetic field (over 7 T) (Donatelli et al., 2018; Henning, 2018; Turing, 2019).

Molecular imaging enables the quantitative characterization and measurement of biological diagnosis at the cellular and molecular level, which will inevitably advance the modern and future medical imaging and diagnosis (Wu and Shu, 2018; Li and Meade, 2019). However, the current critical issue lies in developing novel and appropriate contrast agents to meet the biological compatibility for different species (Basal et al., 2017). MRI with nanoparticle contrast agent offers one desired solution to realize molecular imaging. However, the poor sensitivity of MRI limits its wide application in clinics. Efforts can be made toward integrating the varied modalities/strengths of different instruments to avoid the problems existed in an individual instrument. Alternatively, interdisciplinary cooperation among different subjects should be strengthened to resolve the limited resolution of imaging, because molecular imaging requires the joint research of radiology, materials science and ultrasonic medicine.

To sum it up, multimodal molecular imaging agents and specific targeted molecular imaging agent will be both expected in the molecular imaging in future clinic application. With the aid of AI, a major breakthrough can be expected in multimodal molecular imaging for molecular biology clinics, despite molecular imaging combined with AI learning is still at the initial stage.

AUTHOR CONTRIBUTIONS

The author confirms being the sole contributor of this work and has approved it for publication.

FUNDING

REFERENCES

Anwaier, G., Chen, C., Cao, Y., and Qi, R. (2017). A review of molecular imaging of atherosclerosis and the potential application of dendrimer in imaging of plaque. *Int. J. Nanomed.* 12, 7681–7693. doi: 10.2147/IJN.S1 42385

Banerjee, A., Blasiak, B., Pasquier, E., Tomanek, B., and Trudel, S. (2017). Synthesis, characterization, and evaluation of PEGylated first-row transition metal ferrite nanoparticles as T2 contrast agents for high-field MRI. *RSC Adv.* 7, 38125–38134. doi: 10.1039/C7RA05495E

Bao, Y., Sherwood, J. A., and Sun, Z. (2018). Magnetic iron oxide nanoparticles as T1 contrast agents for magnetic resonance imaging. *J. Mater. Chem. C* 6, 1280–1290. doi: 10.1039/C7TC05854C

Basal, L. A., and Allen, M. J. (2018). Synthesis, characterization, and handling of Eu(II)-containing complexes for molecular imaging applications. *Front. Chem.* 6:65. doi: 10.3389/fchem.2018.00065

Basal, L. A., Yan, Y., Shen, Y., Haacke, E. M., Mehrmohammadi, M., and Allen, M. J. (2017). Oxidation-responsive, Eu(II/III)-based, multimodal contrast agent for magnetic resonance and photoacoustic imaging. *ACS Omega* 2, 800–805. doi: 10.1021/acsomega.6b00514

Bernal, J., Kushibar, K., Asfaw, D. S., Valverde, S., Oliver, A., Marti, R., et al. (2019). Deep convolutional neural networks for brain image analysis on magnetic resonance imaging: a review. *Artif. Intell. Med.* 95, 64–81. doi: 10.1016/j.artmed.2018.08.008

Biju, S., Gallo, J., Banobre-Lopez, M., Manshian, B. B., Soenen, S. J., Himmelreich, U., et al. (2018). A magnetic chameleon: biocompatible lanthanide fluoride nanoparticles with magnetic field dependent tunable contrast properties as a versatile contrast agent for low to ultrahigh field MRI and optical imaging in biological window. *Chemistry Eur. J.* 24, 7388–7397. doi: 10.1002/chem.201800283

Bobo, D., Robinson, K. J., Islam, J., Thurecht, K. J., and Corrie, S. R. (2016). Nanoparticle-based medicines: a review of FDA-approved materials and clinical trials to date. *Pharm. Res.* 33, 2373–2387. doi: 10.1007/s11095-016-1958-5

Botar, R., Molnar, E., Trencsenyi, G., Kiss, J., Kalman, F. K., and Tircso, G. (2020). Stable and inert Mn(II)-based and pH-responsive contrast agents. *J. Am. Chem. Soc.* 142, 1662–1666. doi: 10.1021/jacs.9b 09407

Bridot, J. L., Laurent, A.C., Rivieire, C., Billotey, C., Hiba, B., Janier, M., et al. (2007). Hybrid gadolinium oxide nanoparticles: multimodal contrast agents for *in vivo* imaging. *J. Am. Chem. Soc.* 129, 5076–5084. doi: 10.1021/ja068356j

Busch, H. V. (2019). Artifical intelligence for MRI. *Product News-Magnetom Flash* 74, 94–97. Available online at: https://www.siemens-healthineers.com/en-au/magnetic-resonance-imaging/news/artificial-intelligence-for-mri.html

Busquets, M. A., Estelrich, J., and Sánchez-Martín, M. J. (2015). Nanoparticles in magnetic resonance imaging: from simple to dual contrast agents. *Int. J. Nanomed.* 10, 1727–1741. doi: 10.2147/IJN.S76501

Cai, W., and Chen, X. (2007). Nanoplatforms for targeted molecular imaging in living subjects. *Small* 3, 1840–1854. doi: 10.1002/smll.200700351

Chang, C., Raven, E. P., and Duyn, J. H. (2016). Brain-heart interactions: challenges and opportunities with functional magnetic resonance imaging at ultra-high field. *Philos. Trans. A Math. Phys. Eng. Sci.* 374:20150188. doi: 10.1098/rsta.2015.0188

Chang, X., Zhang, M., Wang, C., Zhang, J., Wu, H., and Yang, S. (2020). Graphene oxide/BaHoF5/PEG nanocomposite for dual-modal imaging and heat shock protein inhibitor-sensitized tumor photothermal therapy. *Carbon* 158, 372–385. doi: 10.1016/j.carbon.2019.10.105

Chaudhari, A. S., Fang, Z., Kogan, F., Wood, J., Stevens, K. J., Gibbons, E. K., et al. (2018). Super-resolution musculoskeletal MRI using deep learning. *Magn. Reson. Med.* 80, 2139–2154. doi: 10.1002/mrm.27178

Chen, G., Roy, I., Yang, C., and Prasad, P. N. (2016). Nanochemistry and nanomedicine for nanoparticle-based diagnostics and therapy. *Chem. Rev.* 116, 2826–2885. doi: 10.1021/acs.chemrev.5b00148

Chen, Z. Y., Wang, Y. X., Lin, Y., Zhang, J. S., Yang, F., Zhou, Q. L., et al. (2014). Advance of molecular imaging technology and targeted imaging agent in imaging and therapy. *Biomed. Res. Int.* 2014:819324. doi: 10.1155/2014/819324

Cho, Z. H., Son, Y. D., Choi, E. J., Kim, H. K., Kim, J. H., Lee, S. Y., et al. (2013). *In vivo* human brain molecular imaging with a brain-dedicated PET/MRI system. *Magn. Reson. Mater. Phy.* 26, 71–79. doi: 10.1007/s10334-012-0329-4

Cho, Z. H., Son, Y. D., Kim, H. K., Kim, K. N., Oh, S. H., Han, J. Y., et al. (2008). A fusion PET-MRI system with a high-resolution research tomograph-PET and ultra-high field 7.0 T-MRI for the molecular-genetic imaging of the brain. *Proteomics* 8, 1302–1323. doi: 10.1002/pmic.200700744

Clough, T. J., Jiang, L., Wong, K. L., and Long, N. J. (2019). Ligand design strategies to increase stability of gadolinium-based magnetic resonance imaging contrast agents. *Nat. Commun.* 10:1420. doi: 10.1038/s41467-019-09342-3

Codari, M., Schiaffino, S., Sardanelli, F., and Trimboli, R. M. (2019). Artificial intelligence for breast MRI in 2008-2018: a systematic mapping review. *AJR Am. J. Roentgenol.* 212, 280–292. doi: 10.2214/AJR.18.20389

Craig, S. E. L., Wright, J., Sloan, A. E., and Brady-Kalnay, S. M. (2016). Fluorescent-guided surgical resection of glioma with targeted molecular imaging agents: a literature review. *World Neurosurg.* 90, 154–163. doi: 10.1016/j.wneu.2016.02.060

Csajbok, E., Banyai, I., Vander Elst, L., Muller, R. N., Zhou, W., and Peters, J. A. (2005). Gadolinium(III)-loaded nanoparticulate zeolites as potential high-field MRI contrast agents: relationship between structure and relaxivity. *Chemistry* 11, 4799–4807. doi: 10.1002/chem.200500039

Dammes, N., and Peer, D. (2020). Monoclonal antibody-based molecular imaging strategies and theranostic opportunities. *Theranostics* 10, 938–955. doi: 10.7150/thno.37443

Das, G. K., Johnson, N. J., Cramen, J., Blasiak, B., Latta, P., Tomanek, B., et al. (2012). $NaDyF_4$ nanoparticles as T_2 contrast agents for ultrahigh field magnetic resonance imaging. *J. Phys. Chem. Lett.* 3, 524–529. doi: 10.1021/jz201664h

Das, G. K., Zhang, Y., D'silva, L., Padmanabhan, P., Heng, B. C., Chye Loo, J. S., et al. (2011). Single-phase Dy_2O_3: Tb^{3+} nanocrystals as dual-modal contrast agent for high field magnetic resonance and optical imaging. *Chem. Mater.* 23, 2439–2446. doi: 10.1021/cm2003066

de Martino, F., Yacoub, E., Kemper, V., Moerel, M., Uludag, K., de Weerd, P., et al. (2018). The impact of ultra-high field MRI on cognitive and computational neuroimaging. *Neuroimage* 168, 366–382. doi: 10.1016/j.neuroimage.2017.03.060

Dearling, J. L., Daka, A., Veiga, N., Peer, D., and Packard, A. B. (2016). Colitis immunoPET: defining target cell populations and optimizing pharmacokinetics. *Inflamm. Bowel Dis.* 22, 529–538. doi: 10.1097/MIB.0000000000000677

Donatelli, G., Ceravolo, R., Frosini, D., Tosetti, M., Bonuccelli, U., and Cosottini, M. (2018). Present and future of ultra-high field MRI in neurodegenerative disorders. *Curr. Neurol. Neurosci. Rep.* 18:31. doi: 10.1007/s11910-018-0841-7

Dong, L., Zhang, P., Lei, P., Song, S., Xu, X., Du, K., et al. (2017). PEGylated GdF_3:Fe nanoparticles as multimodal T_1/T_2-weighted MRI and X-ray CT imaging contrast agents. *ACS Appl. Mater. Interfaces* 9, 20426–20434. doi: 10.1021/acsami.7b04438

Duyn, J. H. (2012). The future of ultra-high field MRI and fMRI for study of the human brain. *Neuroimage* 62, 1241–1248. doi: 10.1016/j.neuroimage.2011.10.065

Dyke, K., Pepes, S. E., Chen, C., Kim, S., Sigurdsson, H. P., Draper, A., et al. (2017). Comparing GABA-dependent physiological measures of inhibition with proton magnetic resonance spectroscopy measurement of GABA using ultra-high-field MRI. *Neuroimage* 152, 360–370. doi: 10.1016/j.neuroimage.2017.03.011

Fan, Q., Cheng, K., Hu, X., Ma, X., Zhang, R., Yang, M., et al. (2014). Transferring biomarker into molecular probe: melanin nanoparticle as a naturally active platform for multimodality imaging. *J. Am. Chem. Soc.* 136, 15185–15194 doi: 10.1021/ja505412p

Faucher, L., Tremblay, M., Lagueux, J., Gossuin, Y., and Fortin, M. A. (2012). Rapid synthesis of PEGylated ultrasmall gadolinium oxide nanoparticles for cell labeling and tracking with MRI. *ACS Appl. Mater. Interfaces* 4, 4506–4515. doi: 10.1021/am3006466

Galluzzi, L., Kepp, O., Vander Heiden, M. G., and Kroemer, G. (2013). Metabolic targets for cancer therapy. *Nat. Rev. Drug Discov.* 12, 829–846. doi: 10.1038/nrd4145

Gao, D., Sheng, Z., Liu, Y., Hu, D., Zhang, J., Zhang, X., et al. (2017). Protein-modified CuS nanotriangles: a potential multimodal nanoplatform for *in vivo* tumor photoacoustic/magnetic resonance dual-modal imaging. *Adv. Healthc Mater.* 6:1601094. doi: 10.1002/adhm.201601094

Gao, D., Zhang, P., Liu, Y., Sheng, Z., Chen, H., and Yuan, Z. (2018). Protein-modified conjugated polymer nanoparticles with strong near-infrared absorption: a novel nanoplatform to design multifunctional nanoprobes for dual-modal photoacoustic and fluorescence imaging. *Nanoscale* 10, 19742–19748. doi: 10.1039/C8NR06197A

Gautam, A., Komal, P., and Singh, R. S. (2019). Future demands for high field MRI diagnostic. *J. Chem. Sci.* 131:89. doi: 10.1007/s12039-019-1668-8

Gong, E., Pauly, J. M., Wintermark, M., and Zaharchuk, G. (2018). Deep learning enables reduced gadolinium dose for contrast-enhanced brain MRI. *J. Magn. Reson. Imaging* 48, 330–340. doi: 10.1002/jmri.25970

Guo, S., Xiao, X., Wang, X., Luo, Q., Zhu, H., Zhang, H., et al. (2019). Reductive microenvironment responsive gadolinium-based polymers as potential safe MRI contrast agents. *Biomater. Sci.* 7, 1919–1932. doi: 10.1039/C8BM01103F

Hai, Z., Ni, Y., Saimi, D., Yang, H., Tong, H., Zhong, K., et al. (2019). γ-lutamyltranspeptidase-triggered intracellular gadolinium nanoparticle formation enhances the T_2-weighted MR contrast of tumor. *Nano Lett.* 19, 2428–2433. doi: 10.1021/acs.nanolett.8b05154

Hametner, S., Dal Bianco, A., Trattnig, S., and Lassmann, H. (2018). Iron related changes in MS lesions and their validity to characterize MS lesion types and dynamics with ultra-high field magnetic resonance imaging. *Brain Pathol.* 28, 743–749. doi: 10.1111/bpa.12643

Harris, M., Biju, S., and Parac-Vogt, T. N. (2019). High-field MRI contrast agents and their synergy with optical imaging: The evolution from single molecule probes towards nano-architectures. *Chemistry Eur. J.* 25, 13838–13847. doi: 10.1002/chem.201901141

Harris, M., Vander Elst, L., Laurent, S., and Parac-Vogt, T. N. (2016). Magnetofluorescent micelles incorporating Dy(III)-DOTA as potential bimodal agents for optical and high field magnetic resonance imaging. *Dalton Trans.* 45, 4791–4801. doi: 10.1039/C5DT04801J

He, S., Song, J., Qu, J., and Cheng, Z. (2018). Crucial breakthrough of second near-infrared biological window fluorophores: design and synthesis toward multimodal imaging and theranostics. *Chem. Soc. Rev.* 47, 4258–4278 doi: 10.1039/C8CS00234G

Henning, A. (2018). Proton and multinuclear magnetic resonance spectroscopy in the human brain at ultra-high field strength: a review. *Neuroimage* 168, 181–198. doi: 10.1016/j.neuroimage.2017.07.017

Hu, D. H., Sheng, Z. H., Zhang, P. F., Yang, D. Z., Liu, S. H., Gong, P., et al. (2013). Hybrid gold-gadolinium nanoclusters for tumor-targeted NIRF/CT/MRI triple-modal imaging *in vivo*. *Nanoscale* 5, 1624–1628. doi: 10.1039/c2nr33543c

Hu, H., Zhang, Y., Shukla, S., Gu, Y., Yu, X., and Steinmetz, N. F. (2017). Dysprosium-modified tobacco mosaic virus nanoparticles for ultra-high-field magnetic resonance and near-infrared fluorescence imaging of prostate cancer. *ACS Nano* 11, 9249–9258. doi: 10.1021/acsnano.7b04472

Huang, J., Bu, L., Xie, J., Chen, K., Cheng, Z., Li, X., et al. (2010). Effects of nanoparticle size on cellular uptake and liver MRI with polyvinylpyrrolidone-coated iron oxide nanoparticles. *ACS Nano* 4, 7151–7160. doi: 10.1021/nn101643u

Huang, J., Guo, M., Ke, H., Zong, C., Ren, B., Liu, G., et al. (2015). Rational design and synthesis of γFe_2O_3 @Au magnetic gold nanoflowers for efficient cancer theranostics. *Adv. Mater.* 27, 5049–5056 doi: 10.1002/adma.201501942

Huelnhagen, T., Paul, K., Ku, M.-C., Serradas Duarte, T., and Niendorf, T. (2017). Myocardial T_2^* mapping with ultrahigh field magnetic resonance: physics and frontier applications. *Front. Phys.* 5:22. doi: 10.3389/fphy.2017.00022

Idisi, D. O., Oke, J. A., Sarma, S., Moloi, S. J., Ray, S. C., Pong, W. F., et al. (2019). Tuning of electronic and magnetic properties of multifunctional r-GO-ATA-Fe_2O_3-composites for magnetic resonance imaging (MRI) contrast agent. *J. Appl. Phys.* 126:035301. doi: 10.1063/1.5099892

Jin, S. M., Lee, H. S., Haque, M. R., Kim, H. N., Kim, H. J., Oh, B. J., et al. (2019). Multi-layer surface modification of pancreatic islets for magnetic resonance imaging using ferumoxytol. *Biomaterials* 214:119224. doi: 10.1016/j.biomaterials.2019.119224

Jung, S. -Y., Gwak, G. -H., Park, J. K., and Oh, J. -M. (2020). Finely crafted quasi-core–shell gadolinium/layered double hydroxide hybrids for switching on/off bimodal CT/MRI contrasting nanodiagnostic platforms. *RSC Adv.* 10, 5838–5844. doi: 10.1039/C9RA08159C

Kim, D.-H., Zeng, H., Ng, T. C., and Brazel, C. S. (2009). T_1 and T_2 relaxivities of succimer-coated $MFe_2^{3+}O_4$ (M = Mn^{2+}, Fe^{2+} and Co^{2+}) inverse spinel ferrites for potential use as phase-contrast agents in medical MRI. *J. Magn. Magn. Mater.* 321, 3899–3904. doi: 10.1016/j.jmmm.2009.07.057

Kim, J., Lee, N., and Hyeon, T. (2017). Recent development of nanoparticles for molecular imaging. *Phil. Trans. R Soc. A Math. Phys. Eng. Sci.* 375:20170022. doi: 10.1098/rsta.2017.0022

Ko, Y. J., Kim, W. J., Kim, K., and Kwon, I. C. (2019). Advances in the strategies for designing receptor-targeted molecular imaging probes for cancer research. *J. Control. Release* 305, 1–17. doi: 10.1016/j.jconrel.2019.04.030

Kubíčková, L., Brázda, P., Veverka, M., Kaman, O., Herynek, V., Vosmanská, M., et al. (2019). Nanomagnets for ultra-high field MRI: magnetic properties

and transverse relaxivity of silica-coated ε-Fe$_2$O$_3$. *J. Magn. Magn. Mater.* 480, 154–163. doi: 10.1016/j.jmmm.2019.02.067

Lee, J. Y., Termsarasab, U., Park, J. H., Lee, S. Y., Ko, S. H., Shim, J. S., et al. (2016). Dual CD44 and folate receptor-targeted nanoparticles for cancer diagnosis and anticancer drug delivery. *J. Control. Release* 236, 38–46. doi: 10.1016/j.jconrel.2016.06.021

Lee, N., Cho, H. R., Oh, M. H., Lee, S. H., Kim, K., Kim, B. H., et al. (2012). Multifunctional Fe$_3$O$_4$/TaO$_x$ core/shell nanoparticles for simultaneous magnetic resonance imaging and X-ray computed tomography. *J. Am. Chem. Soc.* 134, 10309–10312. doi: 10.1021/ja3016582

Lee, S., Xie, J., and Chen, X. (2010). Peptide-based probes for targeted molecular imaging. *Biochemistry* 49, 1364–1376. doi: 10.1021/bi901135x

Lehericy, S., Vaillancourt, D. E., Seppi, K., Monchi, O., Rektorova, I., Antonini, A., et al. (2017). The role of high-field magnetic resonance imaging in parkinsonian disorders: pushing the boundaries forward. *Mov. Disord.* 32, 510–525. doi: 10.1002/mds.26968

Li, D.-Z., Chen, H.-D., Bi, F., and Wang, Z.-X. (2016). Progress of multimodal molecular imaging technology in diagnosis of tumor. *Chinese J. Anal. Chem.* 44, 1609–1618. doi: 10.1016/S1872-2040(16)60966-0

Li, H., and Meade, T. J. (2019). Molecular magnetic resonance imaging with Gd(III)-based contrast agents: challenges and key advances. *J. Am. Chem. Soc.* 141, 17025–17041. doi: 10.1021/jacs.9b09149

Li, H., Parigi, G., Luchinat, C., and Meade, T. J. (2019). Bimodal fluorescence-magnetic resonance contrast agent for apoptosis imaging. *J. Am. Chem. Soc.* 141, 6224–6233. doi: 10.1021/jacs.8b13376

Li, L., Jiang, W., Luo, K., Song, H., Lan, F., Wu, Y., et al. (2013). Superparamagnetic iron oxide nanoparticles as MRI contrast agents for non-invasive stem cell labeling and tracking. *Theranostics* 3, 595–615. doi: 10.7150/thno.5366

Li, X., Kim, J., Yoon, J., and Chen, X. (2017). Cancer-associated, stimuli-driven, turn on theranostics for multimodality imaging and therapy. *Adv. Mater.* 29:1606857. doi: 10.1002/adma.201606857

Liu, Y., Wu, S., Liu, Y., Zhang, H., Zhang, M., Tang, Z., et al. (2020). Cathodic protected Mn^{2+} by Na$_x$WO$_3$ nanorods for stable magnetic resonance imaging-guided tumor photothermal therapy. *Biomaterials* 234:119762. doi: 10.1016/j.biomaterials.2020.119762

Liu, Z., Rong, P., Yu, L., Zhang, X., Yang, C., Guo, F., et al. (2015). Dual-modality non-invasive mapping of sentinel lymph node by photoacoustic and near-infrared fluorescent imaging using dye-loaded mesoporous silica nanoparticles. *Mol. Pharm.* 12, 3119–3128. doi: 10.1021/mp500698b

Lyu, Q., You. C., Shan, H., and Wang, G. (2018). Super-resolution MRI through deep learning. *arXiv Prepr.* arXiv181006776.

Mahmoudi, M., Hosseinkhani, H., Hosseinkhani, M., Boutry, S., Simchi, A., Journeay, W. S., et al. (2011). Magnetic resonance imaging tracking of stem cells *in vivo* using iron oxide nanoparticles as a tool for the advancement of clinical regenerative medicine. *Chem. Rev.* 111, 253–280. doi: 10.1021/cr,1001832

Mahmud, M., Kaiser, M. S., Hussain, A., and Vassanelli, S. (2018). Applications of deep learning and reinforcement learning to biological data. *IEEE Trans. Neural. Netw. Learn. Syst.* 29, 2063–2079. doi: 10.1109/TNNLS.2018.2790388

Marangoni, V. S., Neumann, O., Henderson, L., Kaffes, C. C., Zhang, H., Zhang, R., et al. (2017). Enhancing T$_1$ magnetic resonance imaging contrast with internalized gadolinium(III) in a multilayer nanoparticle. *Proc. Natl. Acad. Sci. U. S. A.* 114, 6960–6965. doi: 10.1073/pnas.1701944114

Marasini, R., Thanh Nguyen, T.D., and Aryal, S. (2020). Integration of gadolinium in nanostructure for contrast enhanced-magnetic resonance imaging. *WIREs Nanomed. Nanobiotechnol.* 12:e1580. doi: 10.1002/wnan.1580

Moser, E., Laistler, E., Schmitt, F., and Kontaxis, G. (2017). Ultra-high field NMR and MRI—the role of magnet technology to increase sensitivity and specificity. *Front. Phys.* 5:33. doi: 10.3389/fphy.2017.00033

Mostapha, M., and Styner, M. (2019). Role of deep learning in infant brain MRI analysis. *Magn. Reson. Imaging* 64, 171–189. doi: 10.1016/j.mri.2019.06.003009

Mulder, M. P. C., Merkx, R., Witting, K. F., Hameed, D. S., El Atmioui, D., Lelieveld, L., et al. (2018). Total chemical synthesis of SUMO and SUMO-based probes for profiling the activity of SUMO-specific proteases. *Angew. Chem. Int. Ed. Engl.* 57, 8958–8962. doi: 10.1002/anie.201803483

Nakada, T. (2007). Clinical application of high and ultra high-field MRI. *Brain Dev.* 29, 325–335. doi: 10.1016/j.braindev.2006.10.005

Nalepa, J., Ribalta Lorenzo, P., Marcinkiewicz, M., Bobek-Billewicz, B., Wawrzyniak, P., Walczak, M., et al. (2020). Fully-automated deep learning-powered system for DCE-MRI analysis of brain tumors. *Artif. Intell. Med.* 102:101769. doi: 10.1016/j.artmed.2019.101769

Ni, D., Bu, W., Ehlerding, E. B., Cai, W., and Shi, J. (2017). Engineering of inorganic nanoparticles as magnetic resonance imaging contrast agents. *Chem. Soc. Rev.* 46, 7438–7468. doi: 10.1039/C7CS00316A

Ni, D., Zhang, J., Bu, W., Zhang, C., Yao, Z., Xing, H., et al. (2016). PEGylated NaHoF$_4$ nanoparticles as contrast agents for both X-ray computed tomography and ultra-high field magnetic resonance imaging. *Biomaterials* 76, 218–225. doi: 10.1016/j.biomaterials.2015.10.063

Norek, M., Kampert, E., Zeitler, U., and Peters, J. A. (2008). Tuning of the size of Dy$_2$O$_3$ nanoparticles for optimal performance as an MRI contrast agent. *J. Am. Chem. Soc.* 130, 5335–5340. doi: 10.1021/ja711492y

O'sullivan, S., Heinsen, H., Grinberg, L. T., Chimelli, L., Amaro, E. Jr., Do Nascimento Saldiva, P. H., et al. (2019). The role of artificial intelligence and machine learning in harmonization of high-resolution post-mortem MRI (virtopsy) with respect to brain microstructure. *Brain Inf.* 6:3. doi: 10.1186/s40708-019-0096-3

Pansare, V. J., Hejazi, S., Faenza, W. J., and Prud'homme, R. K. (2012). Review of long-wavelength optical and NIR imaging materials: contrast agents, fluorophores, and multifunctional nano carriers. *Chem. Mater.* 24, 812–827. doi: 10.1021/cm2028367

Patrick, P. S., Hammersley, J., Loizou, L., Kettunen, M. I., Rodrigues, T. B., Hu, D. E., et al. (2014). Dual-modality gene reporter for *in vivo* imaging. *Proc. Natl. Acad. Sci. U. S. A.* 111, 415–420. doi: 10.1073/pnas.1319000111

Pellico, J., Ellis, C. M., and Davis, J. J. (2019). Nanoparticle-based paramagnetic contrast agents for magnetic resonance imaging. *Contrast Media. Mol. Imaging* 2019, 1–13. doi: 10.1155/2019/1845637

Qin, J., Laurent, S., Jo, Y. S., Roch, A., Mikhaylova, M., Bhujwalla, Z. M., et al. (2007). A high-performance magnetic resonance imaging T$_2$ contrast agent. *Adv. Mater.* 19, 1874–1878. doi: 10.1002/adma.200602326

Rajamanickam, K. (2019). Multimodal molecular imaging strategies using functionalized nano probes. *J. Nanotechnol. Res.* 1, 119–135. doi: 10.26502/jnr.2688-85210010

Raval, S. B., Britton, C. A., Zhao, T., Krishnamurthy, N., Santini, T., Gorantla, V. S., et al. (2017). Ultra-high field upper extremity peripheral nerve and non-contrast enhanced vascular imaging. *PLoS ONE* 12:e0175629. doi: 10.1371/journal.pone.0175629

Rees, J. A., Deblonde, G. J., An, D. D., Ansoborlo, C., Gauny, S. S., and Abergel, R. J. (2018). Evaluating the potential of chelation therapy to prevent and treat gadolinium deposition from MRI contrast agents. *Sci. Rep.* 8:4419. doi: 10.1038/s41598-018-22511-6

Rogosnitzky, M., and Branch, S. (2016). Gadolinium-based contrast agent toxicity: a review of known and proposed mechanisms. *Biometals* 29, 365–376. doi: 10.1007/s10534-016-9931-7

Rosenberg, J. T., Kogot, J. M., Lovingood, D. D., Strouse, G. F., and Grant, S. C. (2010). Intracellular bimodal nanoparticles based on quantum dots for high-field MRI at 21.1 T. *Magn. Reson. Med.* 64, 871–882. doi: 10.1002/mrm.22441

Shan, H., Zhang, Y., Yang, Q., Kruger, U., Kalra, M. K., Sun, L., et al. (2018). 3-D convolutional encoder-decoder network for low-dose CT via transfer learning from a 2-D trained network. *IEEE Trans. Med. Imaging* 37, 1522–1534. doi: 10.1109/TMI.2018.2832217

Shen, D., Wu, G., and Suk, H. I. (2017a). Deep learning in medical image analysis. *Annu. Rev. Biomed. Eng.* 19, 221–248. doi: 10.1146/annurev-bioeng-071516-044442

Shen, Z., Chen, T., Ma, X., Ren, W., Zhou, Z., Zhu, G., et al. (2017b). Multifunctional theranostic nanoparticles based on exceedingly small magnetic iron oxide nanoparticles for T$_1$-weighted magnetic resonance imaging and chemotherapy. *ACS Nano* 11, 10992–11004. doi: 10.1021/acsnano.7b04924

Shen, Z., Song, J., Zhou, Z., Yung, B. C., Aronova, M. A., Li, Y., et al. (2018). Dotted core-shell nanoparticles for T$_1$ -weighted MRI of tumors. *Adv. Mater.* 30:e1803163. doi: 10.1002/adma.201803163

Shen, Z., Wu, A., and Chen, X. (2017c). Iron oxide nanoparticle based contrast agents for magnetic resonance imaging. *Mol. Pharm.* 14, 1352–1364. doi: 10.1021/acs.molpharmaceut.6b00839

Sheth, D., and Giger, M. L. (2019). Artificial intelligence in the interpretation of breast cancer on MRI. *J. Magn. Reson. Imaging*. doi: 10.1002/jmri.26878

Shin, T. H., Choi, Y., Kim, S., and Cheon, J. (2015). Recent advances in magnetic nanoparticle-based multi-modal imaging. *Chem. Soc. Rev.* 44, 4501–4516. doi: 10.1039/C4CS00345D

Song, G., Kenney, M., Chen, Y.S., Zheng, X., Deng, Y., Chen, Z., et al. (2020). Carbon-coated FeCo nanoparticles as sensitive magnetic-particle-imaging tracers with photothermal and magnetothermal properties. *Nat. Biomed. Eng.* 4, 325–334. doi: 10.1038/s41551-019-0506-0

Sosnovik, D. E., Nahrendorf, M., and Weissleder, R. (2007). Molecular magnetic resonance imaging in cardiovascular medicine. *Circulation* 115, 2076–2086. doi: 10.1161/CIRCULATIONAHA.106.658930

Sousa, F., Sanavio, B., Saccani, A., Tang, Y., Zucca, I., Carney, T. M., et al. (2017). Superparamagnetic nanoparticles as high efficiency magnetic resonance imaging T_2 contrast agent. *Bioconjug. Chem.* 28, 161–170. doi: 10.1021/acs.bioconjchem.6b,00577

Thiruppathi, R., Mishra, S., Ganapathy, M., Padmanabhan, P., and Gulyas, B. (2017). Nanoparticle functionalization and its potentials for molecular imaging. *Adv. Sci.* 4:1600279. doi: 10.1002/advs.201600279

Tromsdorf, U. I., Bigall, N. C., Kaul, M. G., Bruns, O. T., Nikolic, M. S., Mollwitz, B. et al. (2007). Size and surface effects on the MRI relaxivity of manganese ferrite nanoparticle contrast agents. *Nano Lett.* 7, 2422–2427. doi: 10.1021/nl071099b

Turing, A. (2019). The journey begins—100daysml. *Mach. Learn. Stat.* Available online at: https://100daysml.com/2019/08/31/the-journey-begins/

Vaughan, J. T., Snyder, C. J., Delabarre, L. J., Bolan, P. J., Tian, J., Bolinger, L., et al. (2009). Whole-body imaging at 7T: preliminary results. *Magn. Reson. Med.* 61, 244–248. doi: 10.1002/mrm.21751

Verwilst, P., Park, S., Yoon, B., and Kim, J. S. (2015). Recent advances in Gd-chelate based bimodal optical/MRI contrast agents. *Chem. Soc. Rev.* 44, 1791–1806. doi: 10.1039/C4CS00336E

Wahsner, J., Gale, E. M., Rodriguez-Rodriguez, A., and Caravan, P. (2019). Chemistry of MRI contrast agents: current challenges and new frontiers. *Chem. Rev.* 119, 957–1057. doi: 10.1021/acs.chemrev.8b,00363

Wang, F. H., Bae, K., Huang, Z. W., and Xue, J. M. (2018). Two-photon graphene quantum dot modified Gd_2O_3 nanocomposites as a dual-mode MRI contrast agent and cell labelling agent. *Nanoscale* 10, 5642–5649. doi: 10.1039/C7NR08068A

Wegmayr, V,. Aitharaju, S., and Buhmann, J. (2018). "Classification of brain MRI with big data and deep 3D convolutional neural networks. Medical imaging 2018," in Computer-Aided Diagnosis, Vol. 10575 (Houston, TX). doi: 10.1117/12.2293719

Werner, E. J., Datta, A., Jocher, C. J., and Raymond, K. N. (2008). High-relaxivity MRI contrast agents: where coordination chemistry meets medical imaging. *Angew. Chem. Int. Ed. Engl.* 47, 8568–8580. doi: 10.1002/anie.200800212

Worden, M., Bruckman, M. A., Kim, M. H., Steinmetz, N. F., Kikkawa, J. M., Laspina, C., et al. (2015). Aqueous synthesis of polyhedral "brick-like" iron oxide nanoparticles for hyperthermia and T_2 MRI contrast enhancement. *J. Mater. Chem. B* 3, 6877–6884. doi: 10.1039/C5TB0 1138H

Wu, L., Jiang, J., Jin, Y., Kallemeijn, W. W., Kuo, C. L., Artola, M., et al. (2017). Activity-based probes for functional interrogation of retaining β-glucuronidases. *Nat. Chem. Biol.* 13, 867–876. doi: 10.1038/nchembio.2395

Wu, M., and Shu, J. (2018). Multimodal molecular imaging: current status and future directions. *Contrast Media Mol. Imaging* 2018:1382183. doi: 10.1155/2018/1382183

Yen, S. K. Janczewski, D., Lakshmi, J. L., Dolmanan, S. B., Tripathy, S., Ho, V. H. B., et al. (2013). Design and synthesis of polymer-functionalized NIR fluorescent dyes-magnetic nanoparticles for bioimaging. *ACS Nano* 7, 6796–6805. doi: 10.1021/nn401734t

Yin, J., Yin, G., Pu, X., Huang, Z., and Yao, D. (2019). Preparation and characterization of peptide modified ultrasmall superparamagnetic iron oxides used as tumor targeting MRI contrast agent. *RSC Adv.* 9, 19397–19407. doi: 10.1039/C.9R.A.02636C

Zaharchuk, G., Gong, E., Wintermark, M., Rubin, D., and Langlotz, C. P. (2018). Deep learning in neuroradiology. *AJNR Am. J. Neuroradiol.* 39, 1776–1784. doi: 10.3174/ajnr.A5543

Zhang, J., Yuan, Y., Gao, M., Han, Z., Chu, C., Li, Y., et al. (2019). Carbon dots as a new class of diamagnetic chemical exchange saturation transfer (diaCEST) MRI contrast agents. *Angew. Chem. Int. Ed. Engl.* 58, 9871–9875. doi: 10.1002/anie.201904722

Zhang, X., Blasiak, B., Marenco, A. J., Trudel, S., Tomanek, B., and van Veggel, F. C. J. M. (2016). Design and regulation of $NaHoF_4$ and $NaDyF_4$ nanoparticles for high-field magnetic resonance imaging. *Chem. Mater.* 28, 3060–3072. doi: 10.1021/acs.chemmater.6b00264

Zhang, Y., Udayakumar, D., Cai, L., Hu, Z., Kapur, P., Kho, E. Y., et al. (2017). Addressing metabolic heterogeneity in clear cell renal cell carcinoma with quantitative dixon MRI. *JCI Insight* 2:e94278. doi: 10.1172/jci.insight.94278

Zhao, M., Beauregard, D.A., Loizou, L., Davletov, B., and Brindle, K. M. (2001). Non-invasive detection of apoptosis using magnetic resonance imaging and a targeted contrast agent. *Nat. Med.* 7, 1241–1244. doi: 10.1038/nm1101-1241

Zhao, Y., Liu, H., Riker, A. I., Fodstad, O., Ledoux, S. P., Wilson, G. L., et al. (2012). Emerging metabolic targets in cancer therapy. *Front. Biosci.* 16:3816. doi: 10.2741/3826

Zhao, Z., Wang, X., Zhang, Z., Zhang, H., Liu, H., Zhu, X., et al. (2015). Real-time monitoring of arsenic trioxide release and delivery by activatable T_1 imaging. *ACS Nano* 9, 2749–2759. doi: 10.1021/nn506640h

Zhao, Z., Zhou, Z., Bao, J., Wang, Z., Hu, J., Chi, X., et al. (2013). Octapod iron oxide nanoparticles as high-performance T_2 contrast agents for magnetic resonance imaging. *Nat. Commun.* 4:2266. doi: 10.1038/ncomms3266

Zheng, X., Wang, Y., Sun, L., Chen, N., Li, L., Shi, S., et al. (2016). TbF_3 nanoparticles as dual-mode contrast agents for ultrahigh field magnetic resonance imaging and X-ray computed tomography. *Nano Res.* 9, 1135–1147. doi: 10.1007/s12274-016-1008-y

Zhou, T., Wu, B., and Xing, D. (2012). Bio-modified Fe_3O_4 core/Au shell nanoparticles for targeting and multimodal imaging of cancer cells. *J. Mater. Chem.* 22, 470–477. doi: 10.1039/C1JM13692E

Zhou, Z., Changqiang, W., Liu, H., Zhu, X., Zhao, Z., Wang, L., et al. (2015a). Surface and interfacial engineering of iron oxide nanoplates for highly efficient magnetic resonance angiography. *ACS Nano* 9, 3012–3022. doi: 10.1021/nn507193f

Zhou, Z., Liu, H., Chi, X., Chen, J., Wang, L., Sun, C., et al. (2015b). A protein-corona-free T_1-T_2 dual-modal contrast agent for accurate imaging of lymphatic tumor metastasis. *ACS Appl. Mater. Interfaces* 7, 28286–28293. doi: 10.1021/acsami.5b08422

Zhou, Z., Yang, L., Gao, J., and Chen, X. (2019). Structure-relaxivity relationships of magnetic nanoparticles for magnetic resonance imaging. *Adv. Mater.* 31:1804567. doi: 10.1002/adma.201804567

Zhu, G., Jiang, B., Tong, L., Xie, Y., Zaharchuk, G., and Wintermark, M. (2019). Applications of deep learning to neuro-imaging techniques. *Front. Neurol.* 10:869. doi: 10.3389/fneur.2019.00869

Zhu, H., and Moser, E. (2017). Editorial: *in vivo* magentic resonance at ultra high field. *Fornt. Phys.* 5:45. doi: 10.3389/fphy.2017. 00045

Zhu, L., Yang, Y., Farquhar, K., Wang, J., Tian, C., Ranville, J., et al. (2016). Surface modification of Gd nanoparticles with pH-responsive block copolymers for use as smart MRI contrast agents. *ACS Appl. Mater. Interfaces* 8, 5040–5050. doi: 10.1021/acsami.5b12463

Zhu, W., Liu, K., Sun, X., Wang, X., Li, Y., Cheng, L., et al. (2015). Mn^{2+}-doped prussian blue nanocubes for bimodal imaging and photothermal therapy with enhanced performance. *ACS Appl. Mater. Interfaces* 7, 11575–11582. doi: 10.1021/acsami.5b02510